THERMODYNAMIC ANALYSIS OF UNSTEADY MHD BOUNDARY LAYER FLOW WITH SLIP OVER A PERMEABLE SURFACE

A thesis presented to the Department of Theoretical & Applied Physics

African University of Science and Technology, Abuja

In partial fulfilment of the requirements for the award

MASTER OF SCIENCE

By

AHMAD MUHAMMAD

Supervised by

Professor Oluwole Daniel Makinde

African University of Science and Technology

www.aust.edu.ng

P.M.B 681, Garki, Abuja F.C.T

Nigeria

June, 2016

CERTIFICATION

The undersigned certify that they have read and hereby recommend for acceptance by the African University of Science & Technology a dissertation titled: "Thermodynamic Analysis of Unsteady MHD Boundary Layer Flow with Slip over a Permeable Surface" in partial fulfilment of the requirements for the degree of Master of Science (Theoretical & Applied Physics) at the African University of Science and Technology.

Principal and Main Supervisor: Professor Oluwole Daniel Makinde

Faculty of Military Science, Stellenbosch University,

Private Bag X2, Saldanha 7395,

South Africa

Signature: …….

24th May, 2016

Date:…….

DECLARATION AND COPYRIGHT

I, Ahmad Muhammad, declare that this dissertation is my own original work and it has not been presented and will not be presented in any other University for a similar or any other degree award.

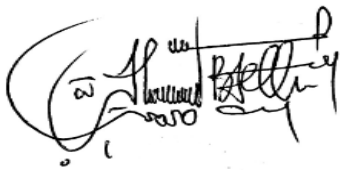

Signature: ……..

ABSTRACT

Magnetohydrodynamics (MHD) boundary layer flow problems have become important in industrial manufacturing processes such as plasma studies, chemical engineering, electrochemistry, polymer processing, petroleum industries, MHD power generator cooling of nuclear reactors, and boundary layer control in aerodynamics. Moreover, permeable surfaces are used for boundary layer control in the filtration processes, and also for a heated body to keep its temperature constant. Suction can be utilized on biological chemical processes to remove reactants while blowing is applied to add reactants in the process and to cool the surface body by its ability to decrease the heat transfer rate. In this thesis, both first and second laws of thermodynamics are employed to investigate the inherent irreversibility in an unsteady hydromagnetic, mixed convective boundary layer flow of an electrically conducting, optically dense fluid, over a permeable vertical surface under the combined influence of thermal radiation, velocity slip, temperature jump, buoyancy force, viscous dissipation, Joule heating and magnetic field. The time-dependent governing partial differential equations are reduced to ordinary differential equations by using appropriate similarity variables. A local similarity solution is obtained numerically using the shooting technique coupled with a fourth order Runge-Kutta Fehlberg integration method. The influence of various thermophysical parameters on velocity and temperature profiles, skin friction, Nusselt number, entropy generation rate and Bejan number, are presented graphically and discussed quantitatively. It is found that velocity slip, surface injection, and temperature jump can successfully reduce entropy generation rate in the presence of an applied magnetic field.

Key terms: magnetohydrodynamics (MHD), boundary value problems (BVPs) initial value problems (IVP)

ACKNOWLEDGEMENT

I am greatly indebted and would like to express my profound gratitude to my thesis advisor Professor Oluwole Daniel Makinde for his exemplary guidance, valuable feedback, tireless assistance and constant encouragement throughout the duration of the work. His valuable suggestions were of immense help throughout my project work. Working under him was an extremely knowledge enhancing experience for me.

I would also like to extend my sincere gratitude to professor Akin-Ojo whose door is always open to address any challenges that I face efficiently and timeously. Besides being generous with his time, he also willingly assists financially and academically. My gratitude also goes to Korand Gufor, Hafeez .Y Hafeez, Irewole Iyomo, Nazifi Uba, Ibrahim Yahaya and many others, whom without which this research would be incomplete.

I would like to use this opportunity to express my profound gratitude to Musa Ahmad Abba, Alhaji Sule Darma and others who have assisted in raising me financially.

Finally,my greatest appreciation goes to the Nelson Mandela Institution for sponsoring my scholarship at A.U.S.T

DEDICATION

I dedicate this to my country, Nigeria

CONTENTS

LIST OF **FIGURES**

LIST OF TABLES

CHAPTER ONE

BACKGROUND STUDY

1.0 Introduction

Fluid Mechanics is the study of fluids either at rest (fluids static) or in motion (fluids dynamics and kinematics) and the subsequent effects of the fluids upon the boundaries which maybe either solid surfaces or interfaces with other fluids. It is worth noting that both gases and liquids are classified as fluids according to Batchelor [37]. Fluids, unlike solids, lack ability to offer sustained resistance to a deforming force. Thus, a fluid is a substance which deforms continuously under the action of shearing forces, however small they may be. Deformation is caused by shearing forces - forces that act tangentially to the surfaces to which they are applied [42].

1.1 Definition of terms

Some relevant fluid properties to be considered in this study are highlighted as follows [37, 42, 45, and 51]:

Pressure: Pressure is the stress at a point in a static fluid. The gradient in pressure often drives a fluid flow, especially in ducts. The unit of pressure is N m^{-2}

Temperature: This is a measure of the internal energy of a fluid. If the temperature differences are strong, heat transfer may be important. The unit is in degree Celsius (^{O}C).

Density: The density of a fluid is its mass per unit volume. Density in liquid is nearly constant. This property aids the classification of fluids as either compressible or incompressible. A fluid is termed compressible if its density varies and increases nearly proportionally to the pressure level. Otherwise it is termed incompressible according to White [51]. The unit of density is kgm^{-3}.

Velocity: The fluid velocity is the rate of displacement of the fluid particles with time. The unit is m/s.

Viscosity: A fluid at rest cannot resist shearing forces and if such forces acts in a fluid which is in contact with solid boundary, the fluid will flow over the boundary in such a way that the particles immediately in contact with the boundary have the same velocity as the boundary

while successive layers of fluid parallel to the boundary move with increasing velocity. Shear stresses opposing the relative motion of these layers are set up and their magnitude depending on the velocity gradient from layer to layer. For fluids obeying Newton's law of viscosity, taking the direction of motion as the x-direction and U as the velocity of the fluid in the x-direction at a distance y from the boundary, the shear stress in the x-direction is given by

$$\tau_x = \mu \frac{dU}{dy} \quad , \tag{1.1}$$

Where the constant μ is called coefficient of dynamic viscosity and its unit is $kgm^{-1}s^{-1}$. The ratio of the coefficient of dynamic viscosity to fluid density is called the kinematic viscosity υ;

$$\upsilon = \frac{\mu}{\rho} \tag{1.2}$$

The viscosity property of fluids aids the classification of fluids into Newtonian or non-Newtonian fluids. Viscosity is associated with collective currents that carry momentum from one region of the fluid to another. Consider a fluid where there is, in addition to thermal agitation of the molecules, a collective movement or current of the whole fluid, for example, water running in a canal or pipe under a pressure difference. Traditionally, viscosity is regarded as the most important material property and any practical study that requires the knowledge of fluid response would automatically turn to the basic understanding of viscosity. In general, the Newtonian model describes the rheological behavior of fluids. The Newtonian model is simply a special case with a constant viscosity. However, viscosity is the strong deformation of fluids. It is the key factor in determining the amount of fluid flowing in channels. It also helps to determine whether the flow regime is laminar, transitional or turbulent. Accurate knowledge of viscosity is very useful for computation of the pressure, velocity, and temperature for a flow system. Viscosity also helps to describe the flow behaviour of shear stress with respect to the rate of deformation of the fluid.

Internal Energy: In thermo-statics, the only energy in a substance is that stored in a system by molecular activity and molecular bonding forces. This is commonly denoted as internal energy. An identified mass of viscous fluid may be viewed as a thermodynamic system that stores various forms of energy. Whenever any form of this fluid is being deformed, it results in an irreversible transformation of mechanical energy into internal or thermal energy. The internal energy of gas includes the energies of translation, rotation, and vibration of the

Molecules as well as, the energy of molecular dissociation and energy of electronic excitation of the molecules. The unit is $Jmol^{-1}$.

Specific Heat Capacity: This refers to the measure of the heat energy required to raise the temperature of one gram of a substance by one degree Celsius. There are two distinctly different experimental conditions under which specific heat capacity is measured. It is measured either under constant pressure condition or under constant volume condition. Typical values of the specific heat of gases are not much different from those of liquids. The unit is $\boldsymbol{Jmol^{-1}K^{-1}}$

Thermal Conductivity: This is the property of fluid that relates the vector rate of heat flow per unit area to the vector gradient of temperature. This proportionality observed experimentally for fluids and solids, is known as Fourier's law of heat conduction, i.e.:

$$q = -k\nabla T. \tag{1.3}$$

The minus sign satisfies the convection that heat flux is positive in the direction of decreasing temperature according to Kay and Crawford [45]. The unit is W m^{-1} K^{-1}.

Table 1.1: Some quantities, symbol and units utilized

Quantity	Symbol	Units
free-stream temperature	T_∞	K
free-stream velocity	u_∞	m/s
kinematic viscosity	υ	m^2/s
dynamic viscosity	μ	kg/m-s
density	ρ	kg/m^3
thermal diffusivity	α	m^2/s
specific heat	c_p	J/kg-K
thermal conductivity	K	W/m-K

Heat Transfer Mechanisms: Heat tends to move from a high-temperature region to a low-temperature region. This heat transfer may occur by the mechanisms of conduction and radiation. In engineering, the term convective heat transfer is used to describe the combined effects of conduction and fluid flow and is regarded as a third mechanism of heat transfer.

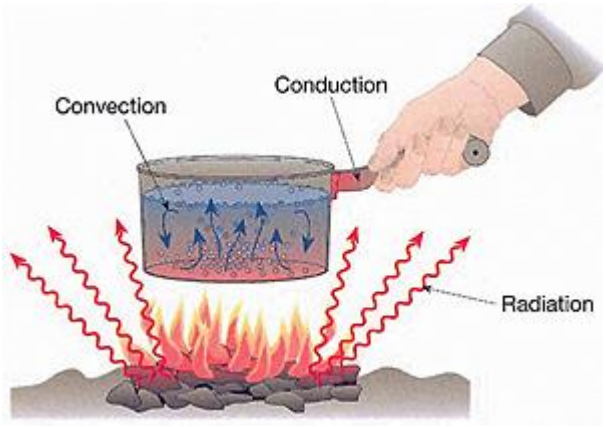

Figure 1.1: Illustration of conduction, convection and radiation heat transfer [45]

Conduction: This is the most significant means of heat transfer in a solid. On a microscopic scale, conduction occurs as hot, rapidly moving or vibrating atoms and molecules interacting with neighbouring atoms and molecules, transferring some of their energy (heat) to these neighbouring atoms. In insulators, the heat flux is carried almost entirely by phonon vibrations. Electrons also conduct electric current through conductive solids, and the thermal and electrical conductivities of most metals have about the same ratio. A good electrical conductor such as copper, usually also conducts heat well. Thermoelectricity is caused by the relationship between electrons, heat fluxes, and electrical currents.

Convection: This is usually the dominant form of heat transfer in liquids and gases. This is a term used to characterize the combined effects of conduction and fluid flow. In convection, enthalpy transfer occurs by the movement of hot or cold portions of the fluid together with heat transfer by conduction. Commonly, an increase in temperature produces a reduction in density. Hence, when water is heated on a stove, hot water from the bottom of the pan rise displacing the colder denser liquid which falls. Mixing and conduction result eventually in a nearly homogeneous density and even temperature. Three types of convection are commonly distinguished, they are free convection, forced convection and mixed convection. Regardless of the particular nature of convection heat transfer process, the rate of heat transfer is given by Newton's law of cooling

$$q'' = h(T_w - T_\infty), \tag{1.4}$$

Where h is the convective heat transfer coefficient, T_w is the geometry surface temperature

Natural or Free Convection: Natural convection is caused by buoyancy forces due to density differences caused by temperature variations in the fluid. At heating, the density change in the boundary layer will cause the fluid to rise and be replaced by cooler fluid that will also heat and rise. This is called free or natural convection. A common example of natural convection is the rise of smoke from a fire. It can be seen in a pot of boiling water in which, the hot and less-dense water on the bottom layer moves upwards in plumes, and the cool and denser water near the top of the pot likewise sinks.

Forced Convection: The fluid movement results from external surface forces such as a fan or a pump i.e. pressure gradient. Forced convection is typically used to increase the rate of heat exchange. Many types of mixing also utilize forced convection to distribute one substance within another. Forced convection also occurs as a by-product of other processes, such as the action of a propeller in a fluid or aerodynamic heating. Fluid radiator systems, and also heating and cooling of parts of the body by blood circulation, are other familiar examples of forced convection.

Mixed Convection: Mixed (combined) convection is a combination of forced and free convections. This is the general case of convection when a flow is determined simultaneously by an outer forcing system (i.e., outer energy supply to the fluid-streamlined body system), and inner volumetric (mass) forces, viz., by the non-uniform density distribution of a fluid medium in a gravity field. The most vivid manifestation of mixed convection is, the motion of the stratified temperature mass of air and water areas of the Earth that are traditionally studied in geophysics. However, mixed convection is found in systems of much smaller scales, i.e., in many engineering devices.

Radiation: This is the only form of heat transfer that can occur in the absence of any form of medium (i.e., through a vacuum). Thermal radiation is a direct result of the movements of atoms and molecules in a material. Since these atoms and molecules are composed of charged particles (protons and electrons), their movements result in the emission of electromagnetic radiation, which carries energy away from the surface. At the same time, the surface is constantly bombarded by radiation from the surroundings, resulting in the transfer of energy to the surface. Since the amount of emitted radiation increases with increasing temperature, a net transfer of energy from higher temperatures to lower temperatures results. The rate of radiation heat exchange between a small surface and large surrounding is given by the expression [6]:

$$Q = \varepsilon\sigma * A(T_s^4 - T_{sur}^4), \tag{1.5}$$

Where ε is the surface emissivity, A is the surface area, σ* is the Stefan-Boltzmann constant, T_s is the absolute temperature of the surface and T_{sur} is the absolute temperature of the surroundings. In differential form, the radiative heat flux within an optically dense medium can be expressed as [6],

$$Q = -\frac{4\sigma *}{3k *}\nabla T^4, \tag{1.6}$$

Where k* the mean absorption coefficient.

The First Law of Thermodynamics: The first law of thermodynamics states that energy is always conserved. This is stated as energy can neither be created nor destroyed; it just changes form. The first law of thermodynamics defines the internal energy as a state function and provides a formal statement of the conservation of energy. However, it provides no information about the direction in which processes can spontaneously occur, that is, the reversibility aspects of thermodynamics processes. For example, it cannot say how cells can perform work while existing in an isothermal environment. It gives no information about the inability of any thermodynamic processes to convert heat into mechanical work with full efficiency, or any insight into why mixtures cannot spontaneously separate, or unmix themselves. An experimentally derived principle to characterize the availability of energy is required to do this. This is precisely the role of the second law of thermodynamics that will be explained next.

The Second Law of Thermodynamics: The second law of thermodynamics establishes the differences in quality between different forms of energy and explains why some processes can spontaneously occur, whereas others cannot. It indicated a trend of change and is usually expressed as an inequality. The second law of thermodynamics has been confirmed by experimental evidence like other physical laws of nature. The second law of thermodynamics defines the fundamental physical quantity entropy as randomized energy state unavailable for direct conversion to work. It also states that all spontaneous processes, both chemical and physical, proceed to maximize entropy, that is, to become more randomized and convert energy into a less available form. A direct consequence of fundamental importance is the implication that at thermodynamic equilibrium, the entropy of a system is at a relative maximum; that is, no further increase in disorder is possible without changing by some external means (such as adding heat)to the thermodynamic state of the system.

A basic corollary of the second law of thermodynamics is the statement that, the sum of the entropy changes of a system and that of the surroundings must always be positive, that is, the universe (the sum of all systems and surroundings) is constrained to become forever more disordered and to proceed towards thermodynamic equilibrium with some absolute maximum value of entropy. The generality of the second law of thermodynamics gives us a powerful means to understand the thermodynamic aspects of real systems through the usage of ideal systems. What makes this new statement of the second law of thermodynamics valuable as a guide to energy policy is, the relationship between entropy and the usefulness of energy. Energy is most useful to us when we can get it to flow from one substance to another, e.g., to warm a house and to conduct work. Useful energy thus must have low entropy so that the second law of thermodynamics will allow transfer or conversions to occur spontaneously.

Energy: This is a scalar quantity which cannot be observed directly but can be recorded and evaluated by indirect measurements. Energy can manifest in various forms. According to Crawford et al. [45], the thermodynamic analysis of energy can be classified into two groups namely:

- Macroscopic forms of energy: This is the energy which an overall system possesses with respect to a reference frame, e.g. Kinetic and potential energies. The macroscopic energy of a system is related to motion and influence of external effects, such as gravity,

magnetism, electricity and surface tension. The energy that the system possesses as a result of its motion relative to some reference form is, kinetic energy. The potential energy of a system is the sum of the gravitational, centrifugal, electrical and magnetic potential energies.

- Microscopic forms of energy: This is the energy that is related to the molecular structure of a system and the degree of molecular activity, and is independent of outside reference frames. The sum of all the microscopic forms of energy of a system is its internal energy. The internal energy of a system depends on the inherent qualities or properties of the materials in the system, such as composition and physical form as well as the environment variables (temperature, pressure, electric field, magnetic field, etc.

Exergy: In thermodynamics, the exergy of a system is the maximum useful work possible during a process that brings the system into equilibrium with a heat reservoir [40]. When the surroundings are the reservoir, exergy is the potential of a system to cause a change as it achieves equilibrium with its environment. Exergy is the energy that is available to be used. After the system and surroundings reach equilibrium, the exergy is zero. Determining exergy was also the first goal of thermodynamics. Energy is never destroyed during a process; it changes from one form to another (see First Law of Thermodynamics). In contrast, exergy accounts for the irreversibility of a process due to an increase in entropy (see Second Law of Thermodynamics). Exergy is always destroyed when a process involves a temperature change. This destruction is proportional to the entropy increase of the system, together with its surroundings. The destroyed Exergy has been called Anergy.

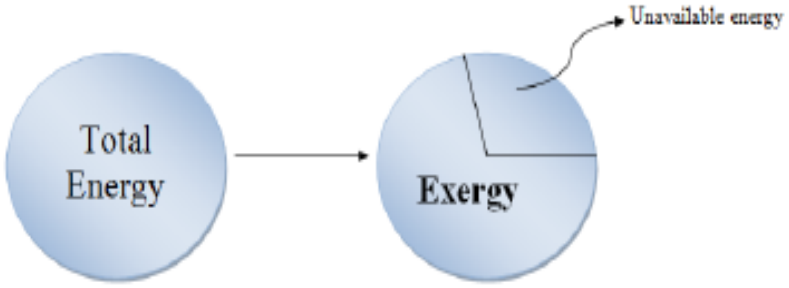

Figure1.2: Illustration of total Energy, Exergy and Anergy of a system

Boundary Layer Flows [31, 34]: A boundary layer is a layer of fluid in the immediate vicinity of a bounding surface where the effects of viscosity are significant. Boundary layer region is the region where the viscous effects and the velocity changes are significant, and the viscid region is the region in which the frictional effects are negligible and the velocity remains essentially constant (i.e. the free stream).In the Earth's atmosphere, the atmospheric boundary layer is the air layer near the ground affected by diurnal heat, moisture or momentum transfer to or from the surface. On a craft wing, the boundary layer is the part of the flow close to the wing, where viscous forces distort the surrounding non-viscous flow. Laminar boundary layers can be loosely classified according to their structure and the circumstances under which they are created. The thin shear layer which develops on an oscillating body is an example of a Stokes boundary layer, while the Blasius boundary layer refers to the well-known similarity solution near an attached flat plate held in an oncoming unidirectional flow. In the theory of heat transfer, a thermal boundary layer occurs. A surface can have multiple types of boundary layers simultaneously. The viscous nature of airflow reduces the local velocities on a surface and is responsible for skin friction. The layer of air over the wing's surface that is slowed down or stopped by viscosity is the boundary layer. Boundary layer flows can be laminar or turbulent in nature.

Laminar Boundary Layer Flow: The laminar boundary is a very smooth flow, while the turbulent boundary layer contains swirls or eddies. The laminar flow creates less skin friction drag than the turbulent flow but is less stable. Boundary layer flow over a wing surface begins as a smooth laminar flow. The laminar boundary layer increases in thickness as the flow continues back from the leading edge. In laminar flow, any exchange of mass or momentum takes place between adjacent layers in microscopic scale which may not be easily observed and consequently, laminar boundary layers are formed for a very small Reynolds number.

Turbulent Boundary Layer Flow: A turbulent boundary layer, on the other hand, is marked by mixing across several layers of it. The mixing is now on a macroscopic scale. Packets of fluid may be seen moving across. Thus there is an exchange of mass, momentum, and energy on a much bigger scale compared to a laminar boundary layer. A turbulent boundary layer forms only at larger Reynolds numbers. The scale of mixing cannot be handled by molecular viscosity alone. Those calculating turbulent flow rely on what is called Turbulence Viscosity or Eddy

Viscosity, which has no exact expression. It has to be modelled. Several models have been developed for this purpose.

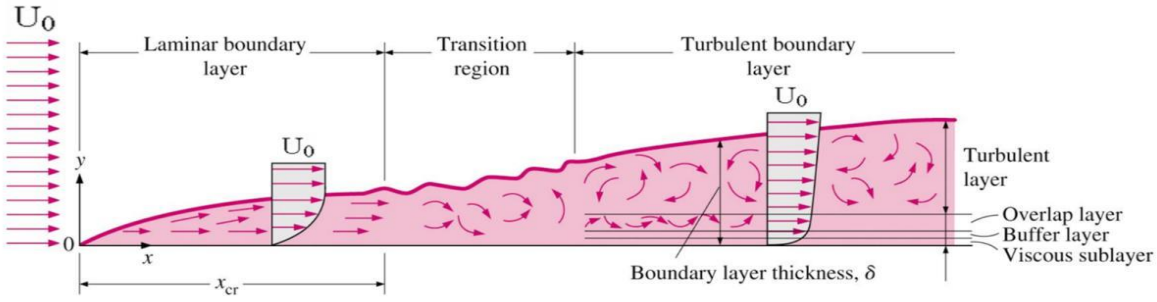

Figure1.3: Laminar boundary layer flow to turbulence boundary layer flow [34]

Magnetohydrodynamics (MHD): This is the study of the magnetic properties of conducting fluids. Examples of such magneto-fluids include plasmas, liquid metals, and salt water or electrolytes. The word magnetohydrodynamics (MHD) is derived from magneto- meaning magnetic field, hydro- meaning water, and -dynamics meaning movement. The field of MHD was initiated by Hannes Alfvén [35] for which he received the Nobel Prize in Physics in 1970. The fundamental concept behind MHD is that magnetic fields can induce currents in a moving conductive fluid, which in turn polarizes the fluid and reciprocally changes the magnetic field itself. The set of equations that describe MHD are a combination of the Navier-Stokes equations of fluid dynamics and Maxwell's equations of electromagnetism. These differential equations must be solved simultaneously, either analytically or numerically.

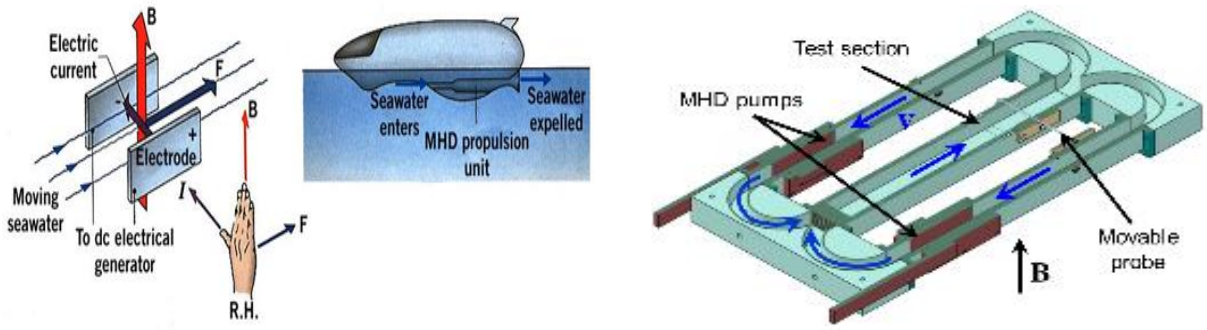

Figure (1.4): Illustration of magnetohydrodynamics [9]

1.2 Problem Statement

Thermodynamic irreversibility in fluid flows and thermal systems is associated with the entropy production that destroys the available energy needed for efficient operation of the system. Consequently, many engineering and industrial devices whose operations depend on fluid flow and heat transfer may not perform at optimal efficiency due to the irreversible loss of energy. In order to achieve entropy generation minimization in fluid flows and thermal systems, it is very important to determine the thermophysical factors that contribute to this inherent irreversibility and control them. This will enhance a better design of the flow and thermal systems for optimal efficiency. Our goal in this thesis is to, examine the thermodynamic inherent irreversibility in an unsteady hydromagnetic boundary layer flow, and heat transfer processes over a slippery permeable surface, in the presence of thermal radiation absorption and buoyancy force. These flow and thermal processes do occur in many engineering and industrial systems devices with hydrophobic open micro-channels such as MHD micro pumps, biological transportation, and drug delivery.

1.3 Study Objectives

The main objectives of the study in this thesis are as follows;

- Derive a nonlinear mathematical model for hydromagnetic boundary layer flow with slip over a permeable surface.
- Solve the nonlinear model numerically using shooting method coupled with fourth order Runge-Kutta integration scheme.
- Determine the effects of various embedded thermophysical parameters on flow characteristics like velocity and temperature profiles, Skin friction and Nusselt number
- Determine the effects of various embedded thermophysical parameters on entropy generation rate, irreversibility ratio and Bejan number.
- Determine the entropy generation minimization condition for optimal performance of the flow system.

1.4 Structure of work

Chapter one is devoted to background information on boundary layer flows of conducting fluids and its important features with respect to the external magnetic field, buoyancy force, thermal radiation absorption, heat transfer and entropy production. Chapter two deals with a review of relevant literature on MHD boundary layer flow with heat transfer, thermal radiation, and entropy generation. The basic (MHD) equations with respect to conservation of mass, momentum and energy balance including Maxwell equations of electromagnetism and the second law of thermodynamics were outlined in Chapter three. In Chapter four, the model problem for entropy generation rate in an unsteady MHD boundary layer flow past a permeable surface with slip, buoyancy force and thermal is formulated, and analysed. The numerical solutions and graphical results are presented and quantitatively discussed in chapter five. This is also followed by a concluding remark. It is hoped that our findings could be useful in improving the liquid transportation design in micro scale MHD systems by reducing the entropy production and improving the exergy of the system.

1.5 Significance of Study

Magnetohydrodynamics (MHD) flow and heat transfer in the presence of slip is an important topic in many engineering branches, especially in the field of microelectrochemical systems (MEMS), such as micro MHD pumps, rapid mixing of biological fluids in biological processes, biological transportation, and drug delivery. The magnetic field applied by generating a Lorentz force can control the electrically conducting fluid flow in a mixing process. However, as most of the applications of biological transportation via an applied magnetic field are in micro/Nano systems .It is necessary to consider the influence of velocity slip at the boundaries. Permeability is another effect that can act as transpiration of the boundaries in microsystems, which is an important aspect of micro-mixing of biological samples. In this process, suction is exerted to remove reactants whereas; injection is exerted to add reactants in the process. The entropy based surface micro-profiling (EBSM) technique is used to reduce energy dissipation in convective heat transfer in microchannels.

1.6 Research Methodology

In our study, the numerical approach in solving model equations with boundary value problems (BVPs) was employed. For this method, we used shooting method together with the fourth order Runge-Kutta-Fehlberg [30]. Shooting method transforms the BVPs into sets of initial value problems (IVP), with certain unknown initial conditions that need to be determined by guessing , after which the fourth order Runge-Kutta-Fehlberg iteration scheme is employed to integrate the set of IVPs until the given boundary conditions are satisfied.

Shooting Method: The shooting method is an iterative algorithm that reformulates the original boundary value problem into a set of initial value problems, with its appropriate initial conditions. The problem requires the solution of the IVP with the initial conditions chosen to approximate the boundary conditions at the end points. If these boundary conditions are not satisfied to the required accuracy, the procedure is repeated again with a new set of initial conditions until the required accuracy is acquired, or a limit to the iteration is reached. The resultant IVP is solved numerically using any appropriate technique for solving the linear ordinary differential equations. In our own case, we used the fourth order Runge-Kutta method, which provides high accuracy results. The solution of the IVP should converge to that of the BVP. The algorithm for the above procedure is implemented in a computer using MATHLAB or MAPLE code. The results are presented usually in graphical form. Consider a two-point boundary value problem:

$$y'' = f(x, y, y'), y(a) = \alpha, y(b) = \beta \tag{1.4}$$

Where, $a < b$ and $x \in [a, b]$. By making initial guess s for $y'(\alpha)$ and denoted by $y(x, s)$. The solution of the initial value problem becomes:

$$y'' = f(x, y, y'), \qquad y(a) = \alpha, \qquad y'(a) = s. \tag{1.5}$$

Introducing the notation $u(x; s)$, $\frac{\partial}{\partial x} y(x; s)$ equation (1.4) can be written as:

$$\frac{\partial}{\partial x} u(x; s) = v(x; s), \; u(a; s) = \alpha,$$

$$\frac{\partial}{\partial x} v(x; s) = f\big(x, u(x; s)\big), \quad v(a; s) = \beta. \tag{1.6}$$

The solution $u(x;s)$ of the initial value problem in (1.6), will coincide with the solution $y(x)$ of the boundary value problem in equation (1.4), we can find a value s such that;

$$\varphi(s) = u(b;s) - \beta = 0. \tag{1.7}$$

Equation (1.7) can be solved using Newton Raphson method if and only if there ζexists$s \in \Re$, such that $\varphi(s) = 0$

Newton Raphson Method: Consider a sequence $\{s_n\}_{n=1}^{\infty}$ generated by:

$$s_{n+1=}s_n - \frac{\varphi(s_n)}{\varphi'(s_n)}. \tag{1.8}$$

Starting by arbitrary chosens_0. To calculate $\varphi'(s_n)$ we introduce new independent variable

$\xi(x;s) = \frac{\partial u(x;s)}{\partial x}$, $\zeta(x;s) = \frac{\partial v(x;s)}{\partial x}$ and differentiate the initial value problem (1.6) with respect to *s* to obtain second IVPs,

$$\frac{\partial \xi(x;s)}{\partial x} = \zeta(x;s), \qquad \zeta(a;s) = 0,$$

$$\frac{\partial \zeta(x;s)}{\partial x} = p(x;s)\xi(x;s) + q(x;s)\zeta(x;s), \zeta(a;s) = 1. \tag{1.9}$$

Where $p(x;s) = \frac{\partial f(x,u(x;s),v(x;s)}{\partial u}$ and$q(x;s) = \frac{\partial f(x,u(x;s),v(x;s)}{\partial v}$. (1.10)

We assign the value$S_n$to $n \geq 0$, then the IVP (1.5) and (1.6) were solved using a numerical method for IVP Such Runge-Kutta in the interval [a, b]. Thus an approximation of $u(b;s)$is obtained to calculate $\varphi(s) = u(b;s) - \beta$ and we also obtain an approximation $\xi(b;s) = \varphi'(s_n)$. The values of $\varphi(s_n)$ and $\varphi'(s_n)$ gives the next Newton-Raphson iterates$S_{n+1}$from equation (1.8). The procedure is repeated until the S_n settle to a fixed number of digits.

Runge-Kutta-Fehlberg Method: One way to guarantee accuracy in the solution of IVPs is to solve the problem twice, using step size and compare answers at mesh points corresponding to large step size. But this requires a significant amount of computation for the smaller step size

and must be repeated, if it is determined that the arrangement is not good enough. Runge-Kutta-Fehlberg method is one way to try to resolve this problem. It has a procedure to determine whether the proper step size is being used. At each step, two different approximations are accepted. If the answers agree to more significant digits than the required, then the step size is increased. Each step requires the following six set of values:

$k_1 = hf(t_n, y_n)$,

$k_2 = hf(t_n, \frac{1}{4}h\ , y_n + \frac{1}{4}k_1)$,

$k_3 = hf(t_n, \frac{3}{8}h\ , y_n + \frac{3}{32}k_1 + \frac{9}{32}k_2)$,

$k_4 = hf(t_n, \frac{12}{13}h\ , y_n + \frac{1932}{2197}k_1 - \frac{7200}{2197}k_2 + \frac{7296}{2197}k_3)$,

$k_5 = hf(t_n, h\ , y_n + \frac{439}{216}k_1 - 8k_2 + \frac{3680}{513}k_3 - \frac{845}{4104}k_4)$,

$k_6 = hf(t_n, \frac{1}{2}h\ , y_n - \frac{8}{27}k_1 - 2k_2 + \frac{3544}{2565}k_3 - \frac{1859}{4104}k_4 - \frac{11}{40}k_5)$,

Then the approximation to the solution of the IVP is made using a fourth order Runge-Kutta method. That is:

$$y_{n+1} = y_n + \frac{25}{216}k_1 + \frac{1408}{2565}k_3 - \frac{2197}{4101}k_4 + \frac{1}{5}k_5 \qquad (1.11)$$

CHAPTER TWO

Literature Review

In 1904 Ludwig Prandtl proposed the boundary layer theory. This theory states that due to the no-slip condition, the velocity on the surface of a stationary body is zero, but the velocity given by inviscid flow theory would be reached within a thin layer called the boundary layer. Since the layer is thin, the velocity gradients are large and the shear stresses are not negligible even when the viscosity is small. The thinness of the boundary layer enables simplifications like rendering the governing equations parabolic and imposing external pressure on the boundary layer. The theory further showed that separation of flow is decided mainly by a streamwise pressure gradient in the external flow. Though originally developed for laminar flow, it was soon extended to turbulent flow. The theory gained acceptance after some years, and helped in the better design of airplanes, engine components and many other equipment involving fluid flow. The boundary layer concept developed rapidly and is now applied in almost all branches of engineering. Blasius [33] presented results for boundary layers over a flat plate in a uniform stream and on a circular cylinder. Prandtl [32] applied the boundary layer concept to heat transfer problems. Detailed history on the development of boundary layer theory with its various applications can be found in Schlichting [34].

Alfven [35] pioneered the study of the interaction between the boundary layer flow of electrically conducting fluid and the magnetic field. The theoretical study of magnetohydromagnetic (MHD) mixed convective flow and heat transfer over a permeable surface, in the presence of slip and radiative heat absorption, appears to be increasingly important due to its various applications in engineering and industry processes. This is notable, especially in the field of micro-electro-mechanical- systems (MEMS), such as micro MHD pumps, micro-electronic devices, rapid mixing of fluids in biological processes, biological transportation, and drug delivery [1-3]. The applied magnetic field generates Lorenz force that controls the electrically conducting fluid flow in a mixing process. Most of the applications of magnetic field in the biological transportation are in the micro/Nanosystems. Therefore, it is necessary to consider the influence of the velocity slip at the boundaries [4]. Surface

permeability is another important aspect in micro-mixing of biological fluid. This enables the transpiration process to take place at the boundaries in a microsystem. In this process, suction is exerted to remove reactants, whereas injection is applied to add reactants in the process [5]. Hydromagnetic flow with heat transfer also play a very vital role in the design of cooling systems for electronic devices, MHD generators, plasma studies, nuclear reactors cooling, geothermal energy extraction, solar energy collection, MHD marine propulsion, electronic packages, thermal insulation, and petroleum reservoirs. Moreover, many processes in engineering do occur at high temperatures and the knowledge of radiative heat transfer becomes very important, particularly in designing pertinent equipment [6-8]. The effects of radiation also become more important when the difference between the surface and the ambient temperature is large. Several excellent studies on hydromagnetic boundary layer flows with heat transfer have been communicated by many authors [9-12].

Mukhopadhyay [13] investigated the slip effects on MHD boundary layer flow by an exponentially stretching sheet with suction/blowing and thermal radiation. The combined effects of variable thermal conductivity, viscous dissipation, and Ohmic heating on MHD natural convection flow of low Prandtl fluid over an inclined porous plate was studied by Sharma and Singh [14]. Kim [15] reported a numerical solution for the unsteady MHD convective heat transfer past a semi-infinite vertical porous moving plate with variable suction. Bhattacharyya and Layek [16] discussed the problem of chemically reactive solute distribution in hydromagnetic boundary layer flow over a permeable stretching sheet with suction or blowing. The combined effects of velocity slip and temperature jump on hydromagnetic boundary layer flow of an electrically conducting fluid over a porous shrinking surface was numerically investigated by Zheng *et al.* [17].

Meanwhile, the recent trend in the study of fluid flow with heat transfer characteristics is related to the concept of entropy generation minimization. The foundation of knowledge of entropy production goes back to Clausius and Kelvin's [18] studies on the irreversible aspects of the second law of thermodynamics. Entropy generation is associated with thermodynamic irreversibility, and is common to all types of fluid flow with heat transfer processes. Efficient utilization of energy is the primary objective in the design of any thermodynamic system. This can be achieved by minimizing entropy generation in the system, since entropy production

destroys the available energy. The core interest in thermodynamic irreversibility analysis is to determine the factors responsible for the entropy generation and minimise their effects, in order to avoid the energy losses and fully utilize the available energy resources. Such information can also be employed to improve the design of flow and thermal systems for efficient operation. Bejan [19, 20] introduced the theoretical concept of entropy generation minimization with respect to fluid flow with heat transfer characteristics. Thereafter, several researchers [21-24, 36, 39, 43, 44, 46-50, 52] have investigated the problem under various physical situations. They showed that the pertinent flow parameters might be chosen in order to minimize entropy generation inside the system. Chinyoka and Makinde [25] numerically studied the entropy generation rate in an unsteady porous channel flow with Navier slip and convective cooling.

Mahmud and Frazer [26] studied the effect of viscous dissipation on entropy generation characteristic inside a porous channel. Makinde and Beg [27] applied the second law analysis to the problem of inherent irreversibility in a reactive hydromagnetic channel flow. The entropy generation rate in hydromagnetic boundary layer flow over a convectively heated flat surface was analysed by Makinde [28]. Yazdi *et al.* [29] numerically investigated the problem of entropy production in an electrically conducting fluid flowing over open parallel microchannels embedded in a micro-patterned permeable surface in the presence of an externally imposed magnetic field. They reported that microchannels embedded in a micro-patterned permeable surface can successfully reduce entropy generation in the presence of an applied magnetic field. There have been numerous analytical or numerical solutions in the literature developed particularly for entropy generation analysis of boundary layer flow. However, to the best of our knowledge, no research has been done yet to analyse the combined effects of velocity slip, buoyancy force, temperature jump, thermal radiation absorption, viscous and Joule heating on local entropy production in unsteady MHD fluid flow with heat transfer over a permeable surface. Therefore, our objective is to tackle this problem numerically using shooting technique coupled with Runge-Kutta-Fehlberg integration method. This study essentially extends the earlier work of Makinde [21] and Yazdi *et al.* [29] to unsteady MHD boundary layer flow with inclusion of thermal radiation, suction/injection, temperature jump, buoyancy force and Joule heating. The influence of various thermophysical parameters on the flow velocity, temperature profiles, frictor factor and local Nusselt number, along with the entropy generation rate and Bejan number are discussed with the help of graphs and tables. The presented study may be

applied to a variety of flow and thermal systems, including micro scale systems such as micromixing technologies.

CHAPTER THREE

Derivation of basic fluid equations

In this chapter we shall discuss and derive the basic equations of magneto – hydrodynamic and heat transfer equations. The major equations for the flow structure and heat transfer characteristics are the continuity equation, Navier Stokes equation, the energy, the Maxwell equations of electromagnetism and Entropy generation rate equation based on the second law of thermodynamics.

3.1 The Continuity Equation [34, 42, 51]

Let us apply the principle of Conservation of mass to a fluid flowing in some control volume. Consider an incompressible fluid flowing through some volume bounded by a fixed surface in this flow, a portion of it may coincide with the fixed impermeable boundaries, but another portion of will not. The fundamental requirement for incompressible flow is that the density is constant within an infinitesimal volume, which moves with a flow velocity (outflow taken as positive and inflow taken as negative), therefore, the volumetric in and out flow from the volume V through the surface can be expressed mathematically as

$$\oiint_s \vec{V}.\overrightarrow{e_n}\, ds = 0, \tag{3.1}$$

where $\overrightarrow{e_n}$ is a unit outward normal to the surface S and $\vec{V}$ = (u, v, w) is the velocity of the fluid with components (u, v, w) in the Cartesian coordinate .This equation states that, the net volumetric outflow of the fluid through S is zero or in other words, the net flux through the surface S is zero. it also represents the control volume form of the continuity equation. If we consider V to be infinitesimally small along the flow, then we can apply the divergence theorem and we get:

$$\iiint_v \nabla.V\, dv = 0. \tag{3.2}$$

According to the conservation law, the net mass flow rate out through S must be balanced by the rate of mass decrease within volume. And therefore we have the following equation;

$$\oiint_s \rho\overrightarrow{V}.\overrightarrow{e_n}\,ds + \iiint_v g\,dv = -\frac{dm}{dt}, \tag{3.3}$$

Where g is the generation rate of fluid generated within the volume which is taken to be zero in our case. And therefore we have:

$$\oiint_s \overrightarrow{\rho V}.\overrightarrow{e_n}\,ds = -\frac{dm}{dt}, \tag{3.4}$$

$$\oiint_s \rho\overrightarrow{V}.\overrightarrow{e_n}\,ds = -\frac{d}{dt}\oiint_v(\rho v)\ . \tag{3.5}$$

Applying the divergence theorem to this equation we get,

$$\iiint_v \nabla.(\rho V)\,dv = -\frac{d}{dt}\oiint_v \rho\,dv. \tag{3.6}$$

Re-arranging we have,

$$\iiint_v(\nabla.(\rho V) + \frac{d\rho}{dt})\,dv=0, \tag{3.7}$$

Which will hold for an arbitrary choice of$V$, and therefore we arrive at the continuity equation

$$\nabla.(\rho V) + \frac{d\rho}{dt}=0. \tag{3.8}$$

Since we consider incompressible flow, the density ρ does not vary i.e. its constant throughout the flow and therefore we have

$$\nabla.V = 0 \quad , \tag{3.9}$$

$$\frac{du}{dx} + \frac{dv}{dy} + \frac{dw}{dz} = 0. \tag{3.10}$$

For steady, two-dimensional incompressible flow, we have:

$$\frac{du}{dx} + \frac{dv}{dy} = 0. \tag{3.11}$$

3.2 Navier – Stoke Equations [34, 42, 51]

This is based on the principles of conservation of momentum (Newton's second law of motion) on a fluid in motion. When a fluid is in motion there are different forces that may influence the fluid motion for example gravity, viscosity, pressure force, electrostatic or magnetic force and

many more. To derive the Navier-stokes equation, we apply the principles i.e. Newton's second law to an infinitesimal control volume in a moving fluid with velocity $\vec{}$ .The change in momentum per unit time in the fluid through the control volume in Cartesian coordinate is given by:

$$\iiint_v \frac{D\vec{V}}{Dt}\rho v = \frac{dM}{dt}, \tag{3.12}$$

Where $\frac{D}{Dt}$ is the substantial derivative and $\frac{\partial}{\partial t}$ is the local derivative.

$$\frac{D}{Dt} = \frac{\partial}{\partial t} + (\vec{V}.\nabla). \tag{3.13}$$

We also have what is called the convective derivative $\vec{V}.\nabla$ which in Cartesian coordinate is given by

$$\vec{V}.\nabla = \mathrm{u}\frac{\partial}{\partial x} + v\frac{\partial}{\partial x} + w\frac{\partial}{\partial x}. \tag{3.14}$$

According to conservation law we can equate all forces acting on the fluid and therefore

$$-\iint_s p.\vec{e}_n ds + \iiint_v \rho\vec{g}\, dv + \iiint_v \vec{f}\rho\, dv = \iiint_v \frac{D\vec{V}}{Dt}\rho v, \tag{3.15}$$

Where the first term in left hand side is the pressure force acting in negative normal to the surface s of the control volume for p > 0,$\vec{g}$ is one of the body forces taken into consideration which is directed toward the centre of the earth and $\vec{f}$ is the viscous force per unit mass of the fluid. We can use the divergence theorem to rewrite (3.15) and choosing dv to be infinitesimally small we have

$$-\vec{\nabla}p + \rho\vec{g} + \vec{f}\rho = \frac{D\vec{V}}{Dt}\rho. \tag{3.16}$$

For an incompressible Newtonian fluid it was experimentally found that the viscous force $\vec{f}$ in Cartesian is given by

$$\vec{f} = \nu(\frac{\partial^2\vec{V}}{\partial x^2} + \frac{\partial^2\vec{V}}{\partial y^2} + \frac{\partial^2\vec{V}}{\partial z^2}), \tag{3.17}$$

Withν as the viscosity of the fluid and therefore we can rewrite (3.16) as

$$-\vec{\nabla}p + \rho\vec{g} + \rho\nu(\frac{\partial^2\vec{V}}{\partial x^2} + \frac{\partial^2\vec{V}}{\partial y^2} + \frac{\partial^2\vec{V}}{\partial z^2}) = \frac{D\vec{V}}{Dt}\rho \tag{3.18}$$

The above equation is what is called the Navier-Stokes equation in Cartesian coordinate which we can split into component forms as

$$\left\{\begin{array}{l} \frac{\partial u}{\partial t}+u\frac{\partial u}{\partial x}+v\frac{\partial u}{\partial y}+w\frac{\partial u}{\partial z}=-\frac{1}{\rho}\frac{\partial p}{\partial x}+g_x+\ \nu(\frac{\partial^2 u}{\partial x^2}+\frac{\partial^2 u}{\partial y^2}+\frac{\partial^2 u}{\partial z^2}) \\ \frac{\partial v}{\partial t}+u\frac{\partial v}{\partial x}+v\frac{\partial v}{\partial y}+w\frac{\partial v}{\partial z}=-\frac{1}{\rho}\frac{\partial p}{\partial y}+g_y+\ \nu(\frac{\partial^2 v}{\partial x^2}+\frac{\partial^2 v}{\partial y^2}+\frac{\partial^2 v}{\partial z^2}) \\ \frac{\partial w}{\partial t}+u\frac{\partial w}{\partial x}+v\frac{\partial w}{\partial y}+w\frac{\partial w}{\partial z}=-\frac{1}{\rho}\frac{\partial p}{\partial z}+g_z+\ \nu(\frac{\partial^2 w}{\partial x^2}+\frac{\partial^2 w}{\partial y^2}+\frac{\partial^2 w}{\partial z^2}) \end{array}\right\} \quad (3.19)$$

3.3 Energy Equation [34, 42, 51]

In situations where the fluid may be treated as incompressible with non-negligible temperature variations, the continuity and momentum equations are insufficient to account for all needed variables to characterize the fluid flow, at least one additional equation is required. In some of these instances, the energy equation may be used. In this derivation, we use the fact that work is the dot product of velocity and force and the fact that work and energy are related to each other. The energy equation is, of course, a scalar equation, meaning that it has no particular direction associated with it. The procedure for deriving the energy equation is similar to those presented for the continuity and momentum equations. In this case, the change in energy of the fluid within the control volume is equal to the net thermal energy transferred or outside the control volume plus the rate of work done by external forces. Assume some control volume ΔV in a bulk flow of fluid with some velocity $\vec{V}$ in the Cartesian coordinate system. The change in total energy per unit volume $(\frac{DE}{Dt})$ of the fluid in the control volume is

$$\frac{DE}{Dt}=\frac{\partial E}{\partial t}+\vec{V}.\nabla E. \quad (3.20)$$

The net thermal energy transferred into the control volume is determined by the heat flux$\vec{q}(q_x,q_y,q_z)$ positive for heat going from within the control volume to the surroundings in some given direction. And therefore the total heat Q_h transferred into the control volume is given by

$$Q_h=-(\nabla.\vec{q}). \quad (3.21)$$

The rate of work done per unit volume by surface forces is found by multiplying the stress σ_{ij} by the velocity in a given direction of any face of the control volume , and therefore the rate of work done per unit time being done from all sides is

$$W_m = \nabla(\vec{V}.\vec{\sigma}) , \tag{3.22}$$

Where is the velocity of the fluid given by $\vec{V} = (u, v, w)$ and $\vec{\sigma}$ the principal shear stress at each of the faces given by $\vec{\sigma} = (\vec{\sigma}_x, \vec{\sigma}_y, \vec{\sigma}_z)$

$$\vec{\sigma}_x = (\vec{\sigma}_{xx}, \vec{\sigma}_{xy}, \vec{\sigma}_{xz}) \quad \vec{\sigma}_y = (\vec{\sigma}_{yx}, \vec{\sigma}_{yy}, \vec{\sigma}_{yz}) \quad \vec{\sigma}_z = (\vec{\sigma}_{zx}, \vec{\sigma}_{zy}, \vec{\sigma}_{zz}). \tag{3.23}$$

Amongst the work done by body forces we can include the effect of gravity in the fluid motion. Therefore the work done per unit time per unit volume due to gravitational effects on the fluid motion is

$$W_g = \rho\vec{V}.\vec{g}, \tag{3.24}$$

Where, $\vec{g}$ is the acceleration due to gravity given as $\vec{g} = (g_x, g_y, g_z)$ in Cartesian coordinate system. There could be many other body forces to take into account like the pressure force, the magnetic force etc. and many more, which may be included along in the derivation. But for our own case we apply the conservation law and put terms together. Therefore the conservation law mentioned earlier we will have the below equation

$$\frac{DE}{Dt} = Q_h + W_m + W_g. \tag{3.25}$$

And from (3.20)-(3.25), we can write the above equation as

$$\frac{\partial E}{\partial t} + \vec{V}.\nabla E = -(\nabla.\vec{q}) + \nabla\left(\vec{V}.\vec{\sigma}\right) + \rho\vec{V}.\vec{g}. \tag{3.26}$$

We will now use the Furrier's law of heat conduction that relates heat flow $\vec{q}$ to change in temperature given by

$$\vec{q} = -\vec{K}A(\nabla T), \tag{3.27}$$

Where, $\vec{K}(k_x, k_y, k_z)$ is called the heat conduction coefficient and A is the surface area perpendicular to the direction of and of the faces, T represents the temperature of the flow. From the Zeroth law of thermodynamics, heat flow from a point of higher temperature to the point of

lower temperature. If for example, this is in the x-direction, then $\frac{\partial T}{\partial x}$ is negative. But since heat flow is considered positive when flowing from control volume to the surroundings (meaning for the case of positive x-direction), for q_x to be positive, we need a minus sign as indicated. Thus the heat flow per unit time per unit volume term $Q_h = -(\nabla . \vec{q})$ then becomes$Q_h = \nabla(\vec{K}A(\nabla T))$. For unit area and constant $\vec{K}$ we have

$$Q_h = K\nabla^2 T. \tag{3.28}$$

We therefore can rewrite (3.27) as

$$\frac{\partial E}{\partial t} + \vec{V}.\nabla E = K\nabla^2 T + \nabla\left(\vec{V}.\vec{\sigma}\right) + \rho\vec{V}.\vec{g}. \tag{3.29}$$

The energy $E$of the fluid is expressed in this case as the sum of the absolute thermodynamic internal energy per unit mass, e, and the kinetic energy per unit mass $\frac{V^2}{2}$, ($\vec{V}$is the magnitude of the velocity vector). Thus (3.29) can be written as

$$\frac{\partial(e+\frac{V^2}{2})}{\partial t} + \vec{V}.\nabla(e + \frac{V^2}{2}) = K\nabla^2 T + \nabla\left(\vec{V}.\vec{\sigma}\right) + \rho\vec{V}.\vec{g}, \tag{3.30}$$

Which can be written in component form, for Cartesian can be written as

$$\rho \mathrm{c_p}\left(\frac{\partial T}{\partial t} + u\frac{\partial T}{\partial x} + v\frac{\partial T}{\partial x} + w\frac{\partial T}{\partial x}\right) = K\left(\frac{\partial^2 T}{\partial x^2} + \frac{\partial^2 T}{\partial y^2} + \frac{\partial^2 T}{\partial z^2}\right) + \mu\Phi + R, \tag{3.31}$$

Where $e = c_p T$, c_p is the specific heat at constant pressure and the viscous dissipation functionΦ is given by

$$\Phi = 2\left\{\left(\frac{\partial u}{\partial x}\right)^2 + \left(\frac{\partial v}{\partial y}\right)^2 + \left(\frac{\partial w}{\partial z}\right)^2\right\} + \left(\frac{\partial u}{\partial y} + \frac{\partial v}{\partial x}\right)^2 + \left(\frac{\partial u}{\partial z} + \frac{\partial w}{\partial x}\right)^2 + \left(\frac{\partial v}{\partial z} + \frac{\partial w}{\partial y}\right)^2. \tag{3.32}$$

Where R represents all other energy sources which could be electrical energy, chemical energy etc. below are more general expressions of the energy equations for Newtonian fluids of constant density in some coordinate systems with source terms R. The general case where thermal conductivity may be a function of temperature (vector flux $\vec{q} = \frac{\vec{q}}{A}$ appears in the equations); and the more usual case, where the thermal conductivity is constant.

Microscopic energy balance, in terms of flux; Gibbs notation

$$\rho C_p \left(\frac{\partial T}{\partial t} + \vec{V}.\nabla T\right) = -\nabla \vec{q} + R \tag{3.33}$$

Microscopic energy balance, in terms of flux; Cartesian coordinates is given by

$$\rho C_p \left(\frac{\partial T}{\partial t} + u\frac{\partial T}{\partial x} + v\frac{\partial T}{\partial x} + w\frac{\partial T}{\partial x}\right) = -\left(\frac{\partial q_x}{\partial x} + \frac{\partial q_y}{\partial y} + \frac{\partial q_z}{\partial z}\right) + R \tag{3.34}$$

Microscopic energy balance, in terms of flux; cylindrical coordinates is given by

$$\rho C_p \left(\frac{\partial T}{\partial t} + v_r\frac{\partial T}{\partial r} + \frac{v_\theta}{r}\frac{\partial T}{\partial \theta} + v_z\frac{\partial T}{\partial z}\right) = -\left(\frac{1}{r}\frac{\partial (rq_r)}{\partial r} + \frac{1}{r}\frac{\partial q_\theta}{\partial \theta} + \frac{\partial q_z}{\partial z}\right) + R \tag{3.35}$$

Microscopic energy balance, in terms of flux; spherical coordinates is given by

$$\rho C_p \left(\frac{\partial T}{\partial t} + v_r\frac{\partial T}{\partial r} + \frac{v_\theta}{r}\frac{\partial T}{\partial \theta} + \frac{v_\varphi}{r\,sin\theta}\frac{\partial T}{\partial \varphi}\right) = -\left(\frac{1}{r^2}\frac{\partial (r^2 q_r)}{\partial r} + \frac{1}{r\,sin\theta}\frac{\partial (q_\theta sin\theta)}{\partial \theta} + \frac{1}{r\,sin\theta}\frac{\partial q_\varphi}{\partial \varphi}\right) + R \tag{3.36}$$

And the Fourier's law $\vec{q} = -K\nabla T$ in these coordinate systems can be given as

$$\begin{pmatrix} q_x \\ q_y \\ q_z \end{pmatrix}_{xyz} = \begin{pmatrix} -k\frac{\partial T}{\partial x} \\ -k\frac{\partial T}{\partial y} \\ -k\frac{\partial T}{\partial z} \end{pmatrix}_{xyz} \tag{3.37}$$

Fourier's law of heat conduction, cylindrical coordinate is

$$\begin{pmatrix} q_r \\ q_\varphi \\ q_z \end{pmatrix}_{r\varphi z} = \begin{pmatrix} -k\frac{\partial T}{\partial r} \\ -\frac{k}{r}\frac{\partial T}{\partial \varphi} \\ -k\frac{\partial T}{\partial z} \end{pmatrix}_{r\varphi z} \tag{3.38}$$

Fourier's law of heat conduction, spherical coordinate is given by

$$\begin{pmatrix} q_r \\ q_\theta \\ q_\varphi \end{pmatrix}_{r\theta\varphi} = \begin{pmatrix} -k\frac{\partial T}{\partial r} \\ -\frac{k}{r}\frac{\partial T}{\partial \theta} \\ -\frac{k}{r\,sin\theta}\frac{\partial T}{\partial \varphi} \end{pmatrix}_{r\theta\varphi} \tag{3.39}$$

And the energy equation for systems with constant K are given below in these coordinates

$$\rho C_p \left(\frac{\partial T}{\partial t} + \vec{V}.\nabla T\right) = -k\nabla^2 T + R \tag{3.40}$$

Microscopic energy balance, constant thermal conductivity; Cartesian coordinate

$$\rho C_p \left(\frac{\partial T}{\partial t} + u\frac{\partial T}{\partial x} + v\frac{\partial T}{\partial x} + w\frac{\partial T}{\partial x}\right) = k\left(\frac{\partial^2 T}{\partial x^2} + \frac{\partial^2 T}{\partial y^2} + \frac{\partial^2 T}{\partial z^2}\right) + R \tag{3.41}$$

Microscopic energy balance, constant thermal conductivity; cylindrical coordinates

$$\rho C_p\left(\frac{\partial T}{\partial t}+v_r\frac{\partial T}{\partial r}+\frac{v_\theta}{r}\frac{\partial T}{\partial \theta}+v_z\frac{\partial T}{\partial z}\right)=k\left(\frac{1}{r}\frac{\partial}{\partial r}\left(r\frac{\partial T}{\partial r}\right)+\frac{1}{r^2}\frac{\partial^2 T}{\partial \theta^2}+\frac{\partial^2 T}{\partial z^2}\right)+R \quad (3.42)$$

Microscopic energy balance, constant thermal conductivity; spherical coordinates

$$\rho C_p\left(\frac{\partial T}{\partial t}+v_r\frac{\partial T}{\partial r}+\frac{v_\theta}{r}\frac{\partial T}{\partial \theta}+\frac{v_\varphi}{r\,sin\theta}\frac{\partial T}{\partial \varphi}\right)=k\left(\frac{1}{r^2}\frac{\partial}{\partial r}\left(r^2\frac{\partial T}{\partial r}\right)+\frac{1}{r^2\,sin\theta}\frac{\partial}{\partial \theta}\left(sin\theta\frac{\partial T}{\partial \theta}\right)+\frac{1}{r^2 sin\theta^2}\frac{\partial^2 T}{\partial \varphi^2}\right)+R \quad (3.43)$$

3.4 Lorentz Force [9]

The Lorentz force is the combination of electric and magnetic force on a charged particle due to electromagnetic fields. If a particle of charge q moves with velocity $\vec{V}$in the presence of an electric field $\vec{E}$ and a magnetic field $\vec{B}$, then it will experience a force

$$\vec{F}=q(\vec{E}+(\vec{V}\times\vec{B})). \quad (3.44)$$

For a continuous charge distribution in motion, the Lorentz force equation becomes:

$$d\vec{F}=dq(\vec{E}+(\vec{V}\times\vec{B})), \quad (3.45)$$

Where, $d\vec{F}$ is the force on small piece of charge distribution with charge dq. if both sides of the equation are divided by this small piece of charge distribution dv, the result is

$$\vec{f}=\rho(\vec{E}+(\vec{V}\times\vec{B})), \quad (3.46)$$

Where, $\vec{f}$ is the force density (force per unit volume) and ρ is the charge density (charge per unit volume). Next, the current density corresponding to the motion of the charge continuum is $\vec{J}=\rho\vec{V}$. And therefore the force on the continuous charge distribution is

$$\vec{f}=\rho\vec{E}+(\vec{J}\times\vec{B}). \quad (3.47)$$

The total force on the system is the volume integral over the charge distribution given by;

$$\vec{F}=\iiint(\rho\vec{E}+\vec{J}\times\vec{B})\,dV. \quad (3.48)$$

For limiting cases where the electric field is negligible, the Lorentz force reduces to

$$\vec{F} = \iiint (\vec{J} \times \vec{B})\, dV \tag{3.49}$$

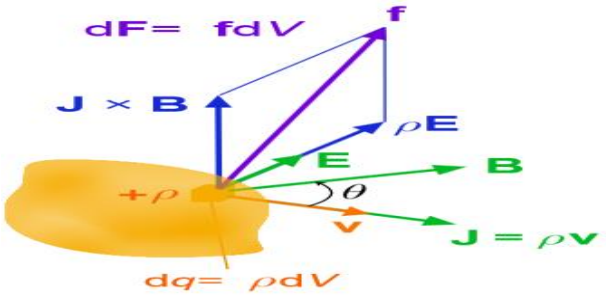

Figure 3.1: The Lorentz force on a continuous charge distribution

The above **Figure** shows the Lorentz force (per unit volume) $\vec{f}$ on a continuous charge distribution in motion with some charge densityρ. The current density $\vec{J}$ corresponds to the motion of the charge element dq in the volume element dV and varies throughout the continuum.

3.5 MHD Equations [9]

Magnetohydrodynamics equations are composed of two main fields namely magnetic (Maxwell's equations of electrodynamics) and the equations of fluid dynamics. In this aspect, we will look at how hydrodynamic equations get to be modified into new set of equations as a result of taking into account the effect of another body force (Lorentz force) on the fluid motion. In the derivation of momentum equation in section (3.2) above, if we assume the fluid flow to be under the influence of some magnetic field of strength$\vec{\mathcal{B}}$. We therefore take into account the electromagnetic body force (called the Lorentz force)$\vec{\mathrm{F}} = (\vec{J} \times \vec{\mathcal{B}})$, and the momentum or Navier-Stokes becomes

$$\rho \frac{D\vec{V}}{Dt} = -\vec{\nabla}p + \rho\vec{g} + \rho\nu\left(\frac{\partial^2\vec{V}}{\partial x^2} + \frac{\partial^2\vec{V}}{\partial y^2} + \frac{\partial^2\vec{V}}{\partial z^2}\right) + (\vec{J} \times \vec{\mathcal{B}}). \tag{3.50}$$

The continuity equation for incompressible fluid such as plasmas, liquid metals etc. will be given as

$$\nabla . V = 0. \tag{3.51}$$

The generalized ohm's law for a slowly movable medium in a magnetic field with velocities less than that of light is

$$\vec{J} = \sigma(\vec{E} + (\vec{V} \times \vec{B})). \tag{3.52}$$

And the Maxwell's equations

$$\vec{\nabla} \times \vec{E} = -\frac{\partial \vec{B}}{\partial t}, \text{(Faraday law of induction)} \tag{3.53}$$

$$\vec{\nabla} \times \vec{B} = \mu_0 \left(\vec{J} + \varepsilon_0 \frac{\partial \vec{E}}{\partial t}\right), \text{(Ampere's circuital law)} \tag{3.54}$$

$$\vec{\nabla}.\vec{B} = 0, \text{(Gauss law of magnetism)} \tag{3.55}$$

$$\vec{\nabla}.\vec{E} = \frac{\rho}{\varepsilon}. \text{ (Gauss law electric field)} \tag{3.56}$$

where $\sigma$is the electrical conductivity of the fluid, $\vec{B}$ is the magnetic induction vector, $\vec{E}$ is the electric field vector, $\vec{J}$ is the electric current density, P is the pressure on the fluid, ν is the kinematic viscosity of the fluid, ρ is the density of the fluid in this case, $\vec{V}$ is the velocity of the fluid ε is the absolute electric permittivity of the fluid and μ is the absolute magnetic permeability of the fluid. If the fluid is not magnetic, then $\mu \approx \mu_0 = 4\pi \cdot 10{-}7\ \mathrm{V} \cdot s/A \cdot m$, where μ_0 is a magnetic permeability in free space.

3.6 Entropy Generation and Second Law [40]

The first part of the second law postulates a thermodynamic state variable, the entropy, is defined by

$$ds = \frac{(d\tilde{q})_{rev}}{T}. \tag{3.57}$$

This definition was originally for a simple, closed system, where $(d\tilde{q})_{rev}$ is the reversible heat transfer that crosses the system's boundary and T is the absolute temperature of the surrounding medium at the boundary. Form this definition and the first law of thermodynamics, the relation for a closed system

$$Tds = dh - \frac{dp}{\rho}\,, \tag{3.58}$$

Was obtained. This equation can be extended to an open system by writing it as

$$Tds = dh - \frac{dp}{\rho} - \sum_{\alpha} \tilde{\mu}_{\alpha} dy_{\alpha}\,. \tag{3.59}$$

If *h* and *p* are held constant, then $-\mu_{\alpha}/T$ provides the entropy change associated with the unit compositional change dy_{α} in species α. For an infinitesimal fluid particle that moves with velocity U but may have diffusion fluxes at its boundary, we can replace the thermodynamic derivatives in equation (3.59) with the substantial derivative to obtain

$$T\frac{Ds}{Dt} = \frac{Dh}{Dt} - \frac{1}{\rho}\frac{Dp}{Dt} - \sum_{\alpha} \tilde{\mu}_{\alpha} \frac{Dy_{\alpha}}{Dt}\,. \tag{3.60}$$

We now use the general form of the energy equation i.e.,

$$\rho\frac{D\bar{h}}{Dt} = \frac{D\bar{p}}{Dt} - \nabla\cdot\vec{q} + \Phi\,, \tag{3.61}$$

Without the over bars symbol to eliminate Dh/Dt, together with the following equation from energy equation

$$\rho\frac{Dy_{\alpha}}{Dt} = \rho\dot{\omega}_{\alpha} - \nabla\cdot\vec{j}_{\alpha} = 0, \alpha = 1,...,N \tag{3.62}$$

to eliminate Dy_{α}/Dt. Equation (3.60) then becomes

$$\rho\frac{Ds}{Dt} = \frac{1}{T}\left(\Phi - \rho\sum_{\alpha}\tilde{\mu}_{\alpha}\dot{\omega}_{\alpha} - \nabla\cdot\vec{q} + \sum_{\alpha}\tilde{\mu}_{\alpha}\nabla\cdot\vec{j}_{\alpha}\right). \tag{3.63}$$

This relation provides the rate of change of entropy of a fluid particle, where part of this change is due to the transport of entropy of a fluid across the system's boundary, as given by $(\bar{d}\bar{q})_{rev}/T$. In

order to focus on entropy transport, we replace $\vec{q}$ by $\vec{q}^*$ and rewrite two terms in the equation (3.63) as

$$-\nabla\cdot\vec{q}+\sum_\alpha\tilde{\mu}_\alpha\cdot\vec{j}_\alpha=-\nabla\cdot\left(\vec{q}^*+\sum_\alpha\tilde{\mu}_\alpha\vec{j}_\alpha\right)+\sum_\alpha\tilde{\mu}_\alpha\nabla\cdot\vec{j}_\alpha$$

$$=-\nabla\cdot\vec{q}^*-\sum_\alpha\vec{j}_\alpha\cdot\nabla\tilde{\mu}_\alpha-\sum_\alpha\tilde{\mu}_\alpha\nabla\cdot\vec{j}_\alpha+\sum_\alpha\tilde{\mu}_\alpha\nabla\cdot\vec{j}_\alpha=-\nabla\cdot\vec{q}*+\sum_\alpha\vec{j}_\alpha\cdot\nabla\tilde{\mu}_\alpha\,, \tag{3.64}$$

To obtain

$$\rho\frac{Ds}{Dt}=\frac{1}{T}\left[\Phi-\sum_\alpha(\rho\tilde{\mu}_\alpha\dot{\omega}_\alpha+\vec{j}_\alpha\cdot\nabla\tilde{\mu}_\alpha)\right]-\frac{1}{T}\nabla\cdot\vec{q}*. \tag{3.65}$$

We introduce $\nabla\cdot(\vec{q}^*/T)$ into equation (3.65) by means of the identity

$$\nabla\cdot\left(\frac{\vec{q}^*}{T}\right)=\frac{1}{T}\nabla\cdot\vec{q}^*+\vec{q}^*.\nabla\frac{1}{T}=\frac{1}{T}\nabla\cdot\vec{q}^*-\frac{1}{T^2}\vec{q}^*\cdot\nabla T$$

to obtain

$$-\frac{1}{T}\nabla\cdot\vec{q}*=-\nabla\cdot\frac{\vec{q}*}{T}-\frac{1}{T^2}\vec{q}*\cdot\nabla T\,. \tag{3.66}$$

Thus, $\nabla\cdot(\vec{q}^*/T)$ corresponds to the entropy transport into or out of the particle. From equation (3.65), we obtain

$$\rho\frac{Ds}{Dt}=\rho\dot{s}_{irr}-\nabla\cdot\frac{\vec{q}*}{T}, \tag{3.67}$$

Where the rate of entropy production per unit volume is given by

$$\rho\dot{s}_{irr}=\frac{1}{T}\left(\Phi-\frac{1}{T}\vec{q}*\cdot\nabla T-\sum_\alpha(\rho\tilde{\mu}_\alpha\dot{\omega}_\alpha+\vec{j}_\alpha\cdot\nabla\tilde{\mu}_\alpha)\right). \tag{3.68}$$

For a reversible process $\dot{s}_{irr}$ = 0 and for an irreversible process $\dot{s}_{irr}$ > 0. The second law of thermodynamics required that $\dot{s}_{irr}$ > 0 for any realizable process. If we suppose that only viscous stresses and conductive heat transfer are present, then equation (3.68) becomes.

$$\rho \dot{s}_{irr} = \frac{1}{T}\left(\Phi - \frac{1}{T}\vec{q}^{\,*} \cdot \nabla T \right). \tag{3.69}$$

Where $\vec{q}$ is now the conductive heat flux. If we further assume Fourier's equation (i.e. $\vec{q}^{\,*} = -\kappa \nabla T$) and a Newtonian fluid, equation (3.69) then becomes

$$\rho \dot{s}_{irr} = \frac{1}{T}\left[\Phi + \frac{\kappa}{T}(\nabla T)^2 \right] \tag{3.70}$$

CHAPTER FOUR

THERMODYNAMICS ANALYSIS OF UNSTEADY MHD MIXED CONVECTION WITH SLIP AND THERMAL RADIATION OVER A PERMEABLE SURFACE

4.1: Introduction

In this chapter we examined the inherent irreversibility in an unsteady mixed convective boundary layer flow of an electrically conducting optically dense incompressible fluid over a permeable vertical surface under the combined influence of thermal radiation, velocity slip, temperature jump, buoyancy force, viscous dissipation, Joule heating and magnetic field. The transient governing partial differential equations for momentum and energy balance are obtained and reduced to ordinary differential equations by using similarity variables. A local similarity solution is obtained numerically using the shooting technique coupled with a fourth order Runge-Kutta Fehlberg integration method. The influence of various thermophysical parameters on velocity and temperature profiles, skin friction, Nusselt number, entropy generation rate and Bejan number are presented graphically and discussed quantitatively

4.2 Model Formulation

We consider an unsteady mixed convective flow of an incompressible, electrically conducting and optically dense fluid over a vertical surface. It is assumed that the plate surface is permeable, fixedand slippery and may be subjected to fluid suction or injection. The x-axis is along the plate surface and y-axis is orthogonal to it. A magnetic field of strengthH_0 is applied normal to the plate surface and the magnetic Reynolds number is assumed to be small so that the induced magnetic field can be neglected in comparison with the applied magnetic field. The physical flow model and coordinate system is shown in **Figure** 4.1 below,

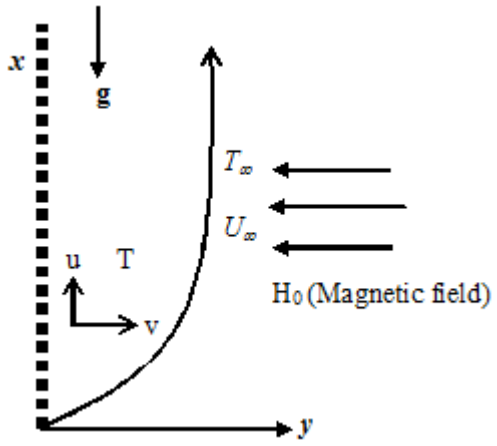

Figure 4.1: Problem geometry

The heat transfer analysis is carried out in the presence of thermal radiation absorption, Joule and viscous heating. Under the usual boundary layer approximations, the governing equations of continuity, momentum with Oberbeck-Boussinesq approximations for the buoyancy forces, and thermal energy can be expressed as [7-9, 13-17]:

$$\frac{\partial v}{\partial y} = 0, \tag{4.1}$$

$$\frac{\partial u}{\partial t} + v\frac{\partial u}{\partial y} = \upsilon\frac{\partial^2 u}{\partial y^2} - \frac{\sigma {H_0}^2}{\rho}(u - U) + g\beta(T - T_\infty) \tag{4.2}$$

$$\frac{\partial T}{\partial t} + v\frac{\partial T}{\partial y} = \alpha\frac{\partial^2 T}{\partial y^2} + \frac{\upsilon}{c_p}(\frac{\partial u}{\partial y})^2 + \frac{\sigma {H_0}^2}{\rho c_p}(u - U)^2 - \frac{1}{\rho c_p}\frac{\partial q_r}{\partial y} \tag{4.3}$$

With the boundary conditions for time $t > 0$ given as,

$$u = L\frac{\partial u}{\partial y},\ T = T_w + m\frac{\partial T}{\partial y},\ \text{ at y = } 0, \tag{4.4}$$

$$u = U, T = T_\infty, \text{ as } y \to \infty \tag{4.5}$$

where (u, v) are the velocity components in the x and y directions respectively, m is the temperature jump, L denotes the velocity slip length, k is the fluid thermal conductivity coefficient, υ is the

kinematic viscosity, ρ is the density, U is the free stream velocity, β is volumetric thermal expansion coefficient, g is the acceleration due to gravity is the temperature, T_w is the plate surface temperature, T_∞ is the free stream temperature, α is the thermal diffusivity and c_p is the specific heat at constant pressure. By using the Rosseland approximation ([6-8]) for thermal radiation in an optically thick layer, the radiative heat flux q_r is given as

$$q_r = -\frac{4\sigma^*}{3k^*}\frac{\partial T^4}{\partial y} \approx -\frac{16\sigma^* T_\infty^3}{3k^*}\frac{\partial T}{\partial y} \tag{4.6}$$

Where $T^4 \cong 4T_\infty^3 T - 3T_\infty^4$ by Taylor series approximation, σ^* is the Stefan–Boltzmann constant, k^* is the mean absorption coefficient. The continuity equation (4.1) shows that the normal velocity v is either constant or a function of time. We therefore choose the time dependent normal velocity as

$$v = -b\left(\frac{\upsilon}{t}\right)^{\frac{1}{2}} \tag{4.7}$$

Where b> 0 is the suction parameter. We introduce the following similarity variables and dimensionless quantities, i.e.

$$\begin{aligned}
&\eta = \frac{y}{2\sqrt{\upsilon t}}, u = Uf(\eta),\ \theta = \frac{T - T_\infty}{T_w - T_\infty},\ \mathrm{Pr} = \frac{\upsilon}{\alpha},\\
&M = \frac{4t\sigma H_0^2}{\rho}, Ec = \frac{U^2}{c_p(T_w - T_\infty)}, \delta = \frac{m}{2\sqrt{\upsilon t}},\\
&\lambda = \frac{L}{2\sqrt{\upsilon t}}, Nr = \frac{16\sigma^* T_\infty^3}{3kk^*}, Gr = \frac{4tg\beta(T_w - T_\infty)}{U}.
\end{aligned} \tag{4.8}$$

Substituting equations (6)-(8) into equations (2)-(5), we obtain

$$f'' + 2(\eta + b)f' - M(f - 1) + Gr\theta = 0 \tag{4.9}$$

$$(1 + Nr)\theta'' + 2\,\mathrm{Pr}(\eta + b)\theta' + \mathrm{Pr}\,Ec\left[(f')^2 + M(f - 1)^2\right] = 0 \tag{4.10}$$

Subject to the boundary conditions;

$$f(0) = \lambda f'(0),\quad \theta(0) = 1 + \delta\theta'(0) \tag{4.11}$$

$$f(\infty)=1,\quad \theta(\infty)=0, \tag{4.12}$$

where prime symbol indicates derivative with respect to η, Pr is the Prandtl number, δ is the temperature jump parameter, M is the magnetic field parameter, Ec is the Eckert number, $Gr$is the local Grashof number, Nr is the thermal radiation parameter and λ is the velocity slip parameter. Moreover, the exact solution for the equations (4.9) to (4.12) exist for the special flow and heat transfer case when M=Gr=Ec=0, and we obtain,

$$f(\eta)=\frac{2\lambda e^{-b^2}+\sqrt{\pi}\left[erf(\eta+b)-erf(b)\right]}{2\lambda e^{-b^2}+\sqrt{\pi}\left[1-erf(b)\right]} \tag{4.13}$$

$$\theta(\eta)=\frac{\sqrt{\pi\,\mathrm{Pr}(1+Nr)}\left[erf\left(\dfrac{\mathrm{Pr}(\eta+b)}{\sqrt{\mathrm{Pr}(1+Nr)}}\right)-1\right]}{\sqrt{\pi\,\mathrm{Pr}(1+Nr)}\left[erf\left(\dfrac{\mathrm{Pr}\,b}{\sqrt{\mathrm{Pr}(1+Nr)}}\right)-1\right]-2\,\mathrm{Pr}\,\delta e^{-\frac{\mathrm{Pr}\,b^2}{1+Nr}}}. \tag{4.14}$$

Other physical quantities of engineering and industrial interest in this study are the skin friction coefficient C_f and the local Nusselt number Nu defined respectively as,

$$C_f=\frac{2t\tau_w}{\rho U\sqrt{\upsilon t}}=f'(0), \tag{4.15}$$

$$Nu=\frac{2q_w\sqrt{\upsilon t}}{k(T_w-T_\infty)}=-(1+Nr)\theta'(0), \tag{4.16}$$

where the τ_w and q_w are the local shear stress and the local heat transfer rate at the permeable surface respectively. They are given as

$$\tau_w=\rho\upsilon\left.\frac{\partial u}{\partial y}\right|_{y=0},\quad q_w=-k\left(1+\frac{16\sigma^* T_\infty^3}{3kk^*}\right)\left.\frac{\partial T}{\partial y}\right|_{y=0}. \tag{4.17}$$

4.3 Entropy Analysis

The inherent irreversibility in a hydromagnetic flow of a conducting fluid over a permeable surface may arise due to the exchange of energy and momentum within the fluid and the solid boundaries.

Consequently, entropy production may occur as a result of fluid friction, magnetic field and heat transfer in the direction of finite temperature gradients. According to Wood [24], the expression for the volumetric entropy generation rate is given as

$$E_G = \underbrace{\frac{k}{T_\infty^2}\left[\left(1+\frac{16\sigma^* T_\infty^3}{3kk^*}\right)\left(\frac{dT}{dy}\right)^2\right]}_{\substack{\text{entropy effects due to}\\ \text{thermal radiation and}\\ \text{heat transfer}}} + \underbrace{\frac{\rho\upsilon}{T_\infty}\left(\frac{du}{dy}\right)^2}_{\substack{\text{entropy effects}\\ \text{due to fluid}\\ \text{friction}}} + \underbrace{\frac{\sigma B_0^2 (u-U)^2}{T_\infty}}_{\substack{\text{entropy effects}\\ \text{due to magnetic}\\ \text{field}}} \tag{4.18}$$

and in dimensionless form, we have

$$Ns = \frac{4T_\infty^2 t\upsilon E_G}{k(T_w - T_\infty)} = (1+Nr)(\theta')^2 + \frac{Br}{\Omega}\left[(f')^2 + M(f-1)^2\right] \tag{4.19}$$

where Br (=$PrEc$) is the Brinkmann number and $\Omega = (T_w\text{-}T_\infty)/T_\infty$ is the temperature difference parameter and $Br\Omega^{-1}$ is referred to as the dimensionless group parameter. $Br\Omega^{-1}$ represents the effect of viscous and Joule heating due to the combined action of fluid friction and magnetic field on the entropy generation rate. The Bejan number is defined as the ratio of heat transfer irreversibility to total irreversibility due to heat transfer, fluid friction and magnetic field for the laminar MHD boundary layer flow. The Bejan number Be is given by [19-24]:

$$Be = \frac{N_1}{Ns} = \frac{1}{1+\Phi} \quad , \tag{4.20}$$

where

$N_1 = (1+Nr)(\theta')^2$, (Is the heat transfer and thermal radiation irreversibility),

$N_2 = \frac{Br}{\Omega}\left[(f')^2 + M(f-1)^2\right]$(Is the fluid friction and magnetic field irreversibility),

$\Phi = \frac{N_2}{N_1}$, (Is the irreversibility ratio).

The Bejan number ranges from 0 to 1, it approaches zero when the entropy generation due to the combined effects of fluid friction and magnetic field is dominant. When Be =0.5 both N_1 and N_2 contribute equally to the entropy generation in the flow process. As Be> 0.5, the irreversibility due

to heat transfer dominate and *Be* = 1 is the limit at which the irreversibility is solely due to heat transfer. Consequently, $0 \leq \Phi \leq 1$ indicates that the irreversibility is primarily due to the heat transfer irreversibility, whereas for $\Phi > 1$ it is due to the sum of the fluid friction and magnetic field irreversibility. The entropy generation rate, *Ns* in equation (4.19) together with Bejan number in equation (4.20) will be used for the evaluation of the present study.

4.4 Numerical procedure

The dimensionless model equations (4.9)-(4.10) together with the boundary conditions (4.11)-(4.12) represent a boundary value problem (BVP) and are transformed into a set of nonlinear first order ordinary differential equations with some unknown initial conditions to be determined by shooting technique. Let,

$$f = y_1\ ,\ f' = y_2, \theta = y_3\ ,\theta' = y_4. \tag{4.21}$$

The governing equations then become

$$\left.\begin{aligned} y_1' = y_2,\ \ y_2' = -2(\eta + b)y_2 + M(y_1 - 1) - Gry_3, \\ y_3' = y_4,\ \ y_4' = -\frac{1}{(1+Nr)}\left[2\,\mathrm{Pr}(\eta + b)y_4 + \mathrm{Pr}\,Ec\left(y_2^2 + M(y_1 - 1)^2\right)\right], \end{aligned}\right\} \tag{4.22}$$

With the corresponding initial conditions as

$$y_1(0) = -\lambda y_2(0),\ \ y_2(0) = a_1,\ \ y_3(0) = 1 + \delta y_4(0),\ \ y_4(0) = a_2. \tag{4.23}$$

The unknown initial conditions a_1, a_2 are first guessed and subsequently determined using Newton-Raphson's method for each set of parameter values with respect to the prescribed boundary conditions. The resulting initial value problem is numerically solved using a fourth order Runge-Kutta-Fehlberg integration scheme [30]. The step size is taken as $\Delta\eta = 0.001$ and the convergence criterion was set to 10^{-6}. In practice, $\eta = \infty$ must be replaced by an approximation $\eta = \eta_{max}$, where η is arbitrary as long as it is chosen large enough so that the prescribed free stream conditions are smoothly satisfied. From the process of numerical computation, we obtain the local skin friction (C_f), the local Nusselt number (*Nu*), the entropy generation rate and the Bejan number as given by equations (4.15) –(4.16) and (4.18)-(4.20).

CHAPTER FIVE

RESULTS, DISCUSSION AND CONCLUSION

In this chapter, we discuss the influence of various thermo physical parameters involved in the present problem on the flow and thermal field along with entropy generation characteristics. For most of the computational results (except where stated), the value of the Prandtl number is chosen to be $Pr = 0.72$, which represents air at 25^0C and one atmospheric pressure. Attention is focused on positive values of the buoyancy parameter (i.e., local thermal Grashof number $Gr > 0$) which corresponds to the cooling problem). The cooling problem is often encountered in engineering applications, for example, in the cooling of electronic components and nuclear reactors. The values of other parameters are fixed arbitrarily for computational purpose. Table 1 shows a comparison between the results obtained from the exact solution of a special flow and heat transfer case when $M = Gr = Ec = 0$ and that of pure numerical approach based on shooting technique coupled with Runge-Kutta-Fehlberg integration scheme. It is noteworthy that the results obtained for shows excellent agreement and this serves as a benchmark for the accuracy of our numerical procedure.

Table 5.1: Comparison between the exact and numerical solutions for Gr = M = Ec= 0, Pr=0.72, Nr=0.1, b=0.1

λ	δ	$f'(0)$ Exact Solution	$-\theta'(0)$ Exact Solution	$f'(0)$ Numerical Solution	$-\theta'(0)$ Numerical Solution
0.1	0.1	1.1179876	0.90730785	1.11798758	0.907307855
0.2	0.2	1.0055665	0.83183482	1.00556650	0.831834828
0.3	0.3	0.9136889	0.76795375	0.91368899	0.767953759
0.4	0.4	0.8371954	0.71318448	0.83719537	0.713184488
0.5	0.5	0.7725203	0.66570727	0.77252033	0.665707278
0.7	0.7	0.6691361	0.58748823	0.66913608	0.587488239

5.1 Velocity Profiles

Figures 5.1-5.9 depict the effects of various thermophysical parameters on the longitudinal velocity profiles and the momentum boundary layer thickness. Generally, the fluid velocity is zero at the permeable stationary plate surface and increases to the prescribed free stream value satisfying the far field boundary condition. In **Figure**s 5.1-5.5, a decrease in the momentum boundary layer thickness accompanies an increase in the magnetic field intensity parameter (M), suction parameter ($b>0$), Grashof number (Gr), radiation absorption parameter (Nr) and Eckert number (Ec) with all profiles tending asymptotically to the free stream value away from the plate. Consequently, the fluid motion in the boundary layer region adjacent to the plate surface increases. This implies that the electrically conducting fluid receives a push from the electromagnetic Lorentz force towards the permeable plate surface. This is the reason why the magnetic field has the potential to move forward an electrically conducting fluid in the micro scale system. Similarly, it is noteworthy that fluid suction, radiation absorption and buoyancy force due to temperature difference also pushes the fluid towards the plate surface in the same manner. **Figure** 5.6 shows the effect of velocity slip on the plate surface. It is noted that an increase in slip parameter λ corresponds to a rise in the fluid velocity adjacent to the surface. In **Figure**s 5.7-5.9, we observed that the momentum boundary layer thickness increases with an increase in fluid injection ($b<0$), temperature jump parameter (δ) and the Prandtl number (Pr). This may be attributed to the combined effects of additional heated fluid entering into the flow regime through injection and a decrease in the fluid thermal diffusivity.

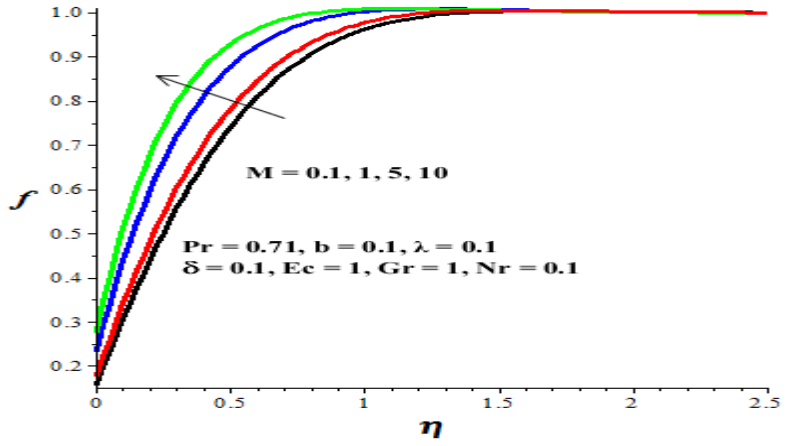

Figure (5.1): Velocity profile with increasing M.

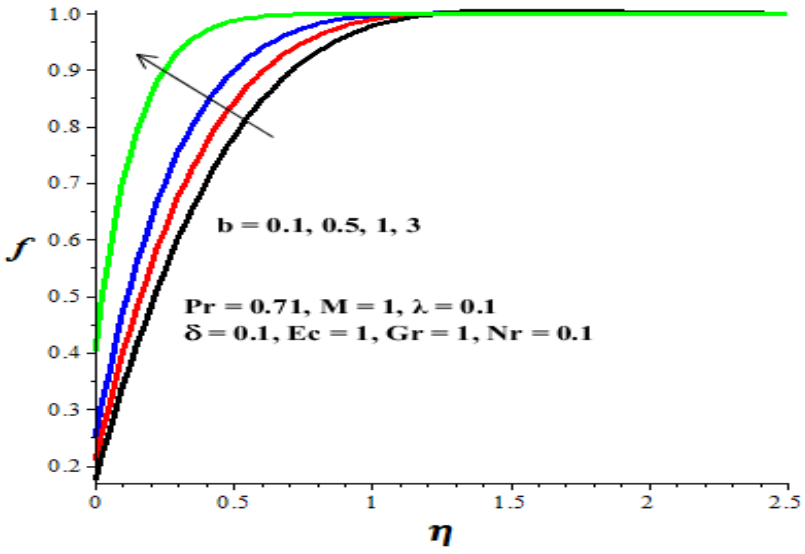

Figure (5.2): Velocity profile with increasing suction (b>0).

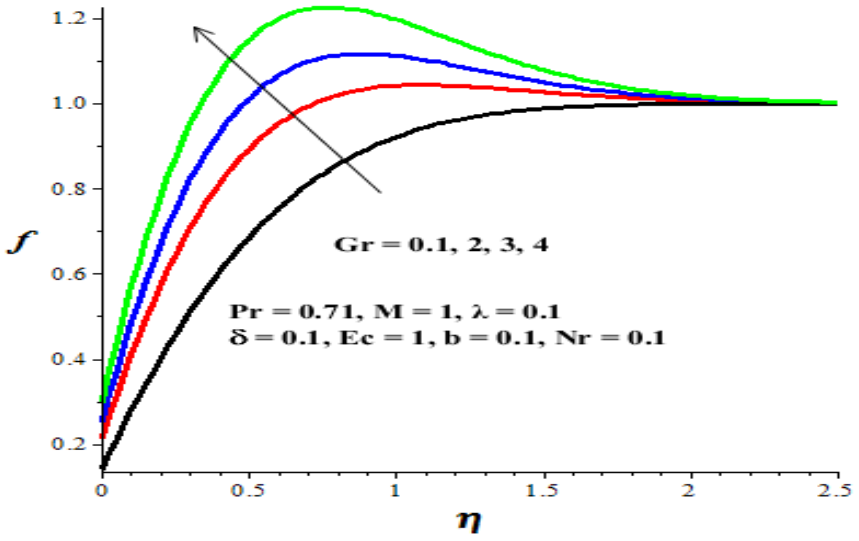

Figure(5.3): Velocity profile with increasing Gr

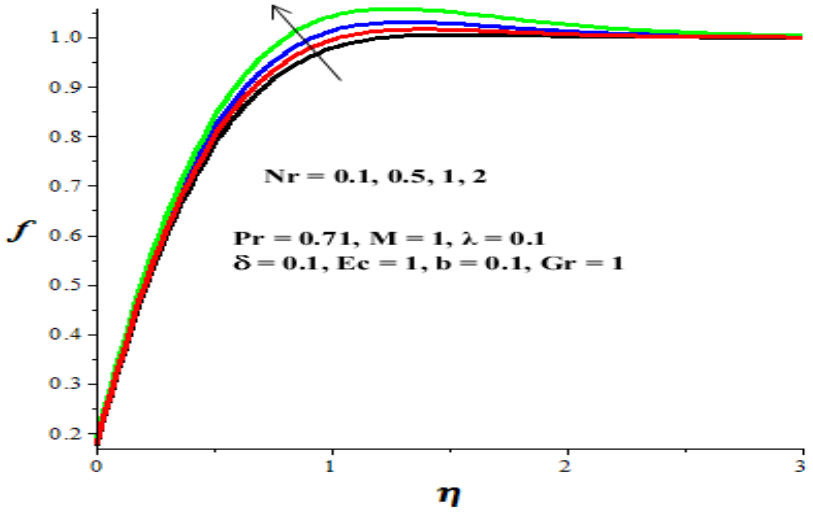

Figure(5.4): Velocity profile with increasing Nr.

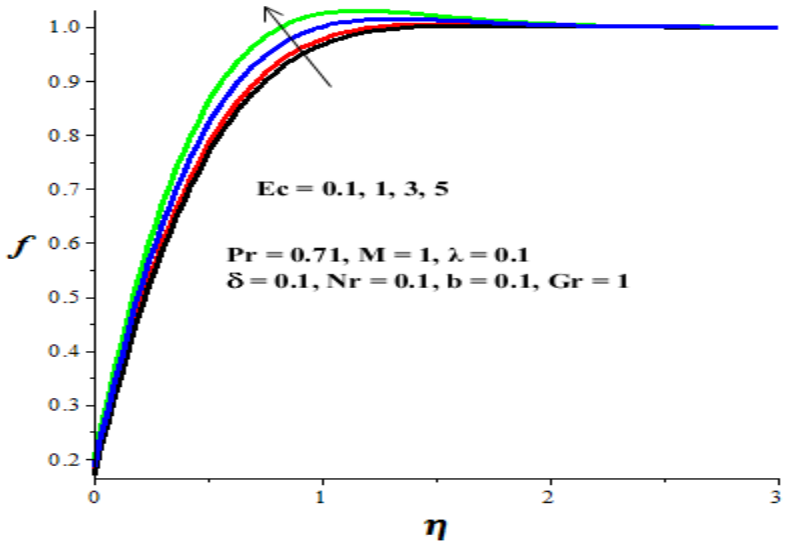

Figure(5.5): Velocity profile with increasing Ec.

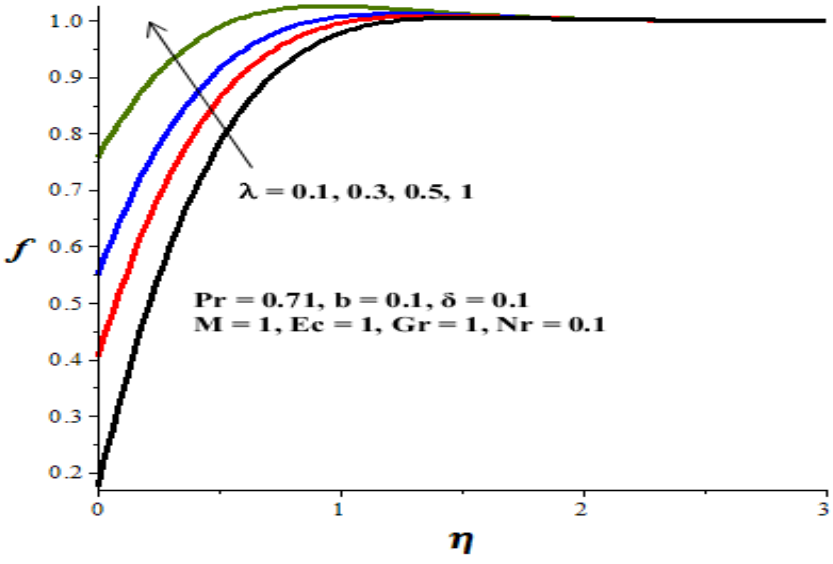

Figure (5.6): Velocity profile with increasing λ.

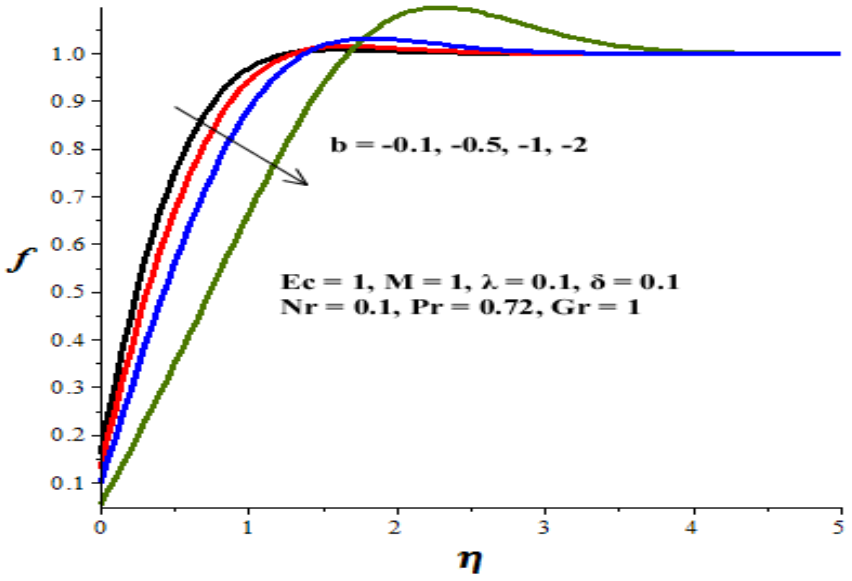

Figure(5.7): Velocity profile with increasing injection (b<0).

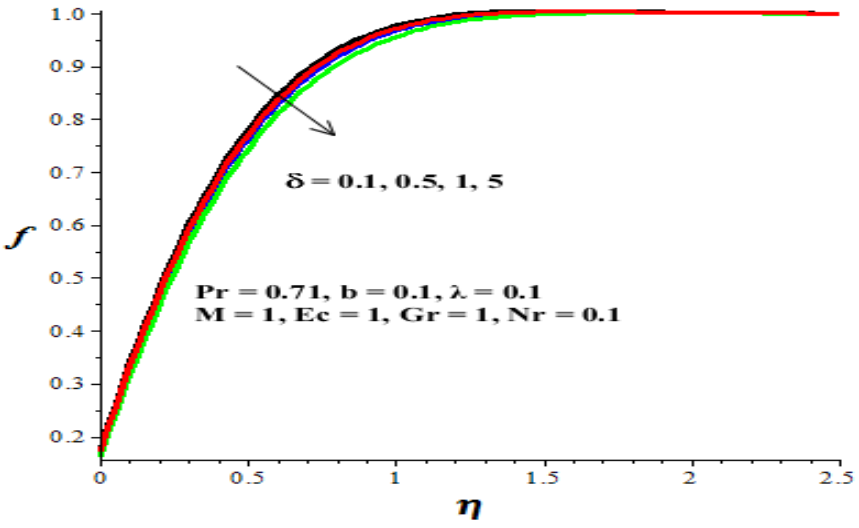

Figure (5.8): Velocity profile with increasingδ.

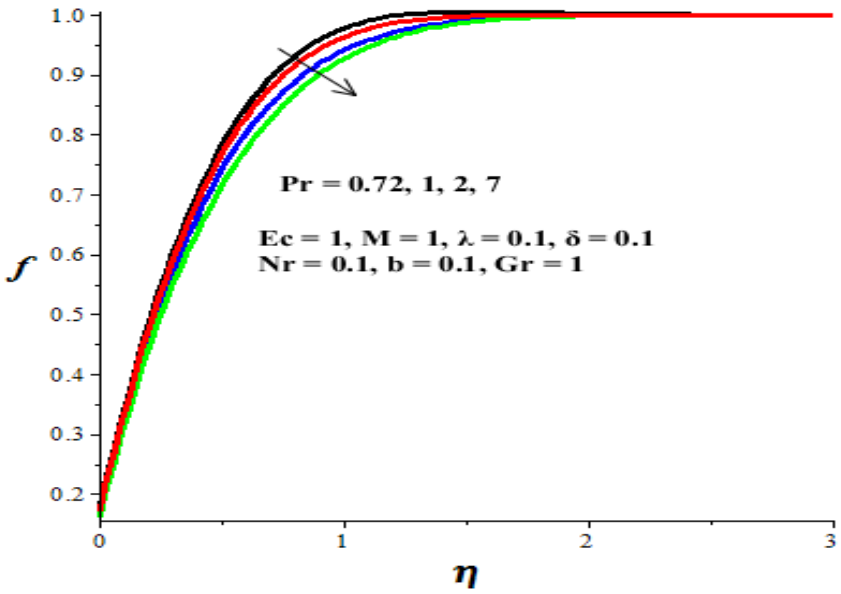

Figure (5.9): Velocity profile with increasing Pr.

5.2 Temperatures Profiles

Figures 5.10-5.18 illustrate the effects of parameters variations on temperature distribution. The fluid temperature is highest at the plate surface and decreases exponentially to the free steam zero value satisfying the prescribed far field condition. We observed that the thermal boundary layer thickness decreases with an increase in velocity slip parameter (λ), temperature jump parameter (δ), fluid suction ($b> 0$) and Prandtl number (Pr) as shown in **Figure**s 5.10-5.13, consequently, the plate surface temperature also decreases. It is important to note that increase in δ correspond to a convective cooling of the plate surface. **Figure** 5.14 depicts a rise in the fluid temperature and thermal boundary layer thickness as the magnetic field intensity parameter increases. The presence of Joule heating (or Lorentz heating due to magnetic field) serves as an additional heat source to the flow system leading to an elevation in the fluid temperature. Similar trend of a rise in the fluid temperature and thermal boundary layer thickness is observed in **Figure**s 5.15-5.18 with an increase in fluid injection parameter ($b< 0$), Grashof number (Gr), radiation absorption parameter (Nr) and Eckert number (Ec). This increase in fluid temperature can be attributed to the absorption of heat by the fluid from the plate surface leading to surface cooling and the viscous dissipation effect that contribute additional heat source to the flow.

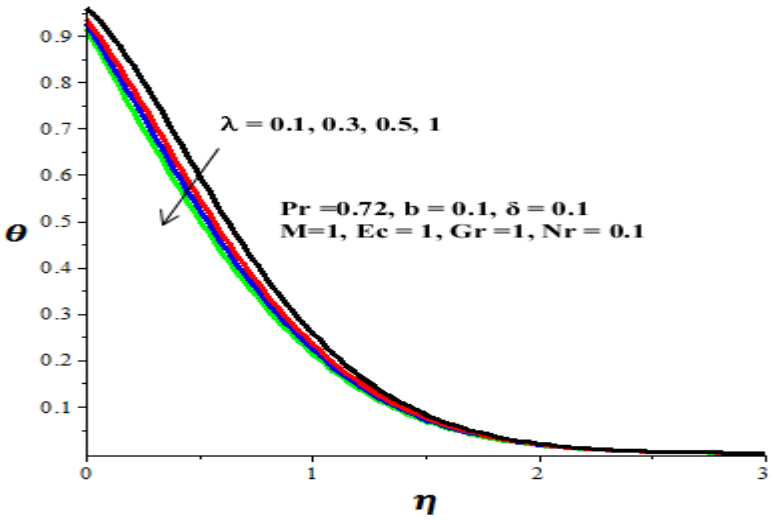

Figure(5.10): Temperature profiles with increasing λ.

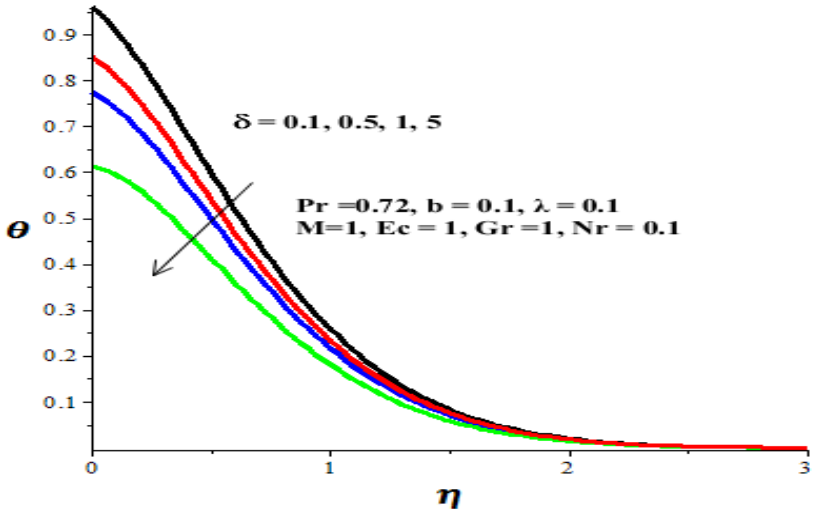

Figure (5.11): Temperature profiles with increasing δ.

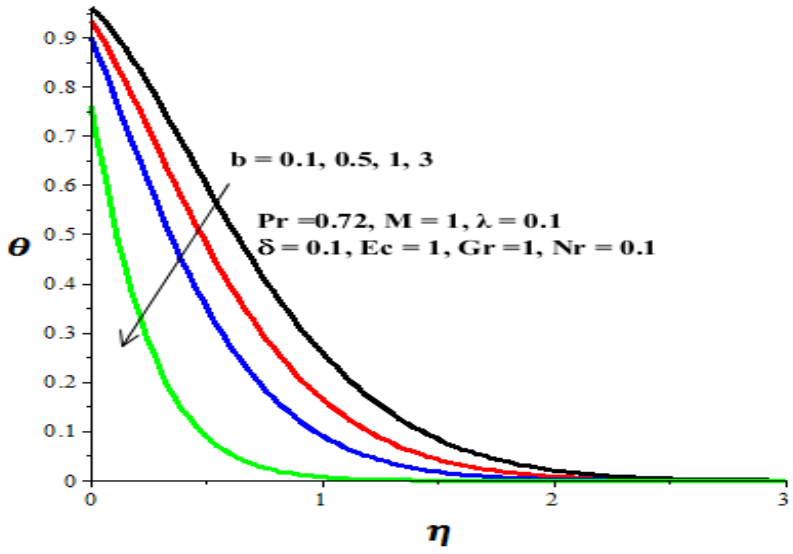

Figure (5.12): Temperature profiles with increasing suction (*b*> 0).

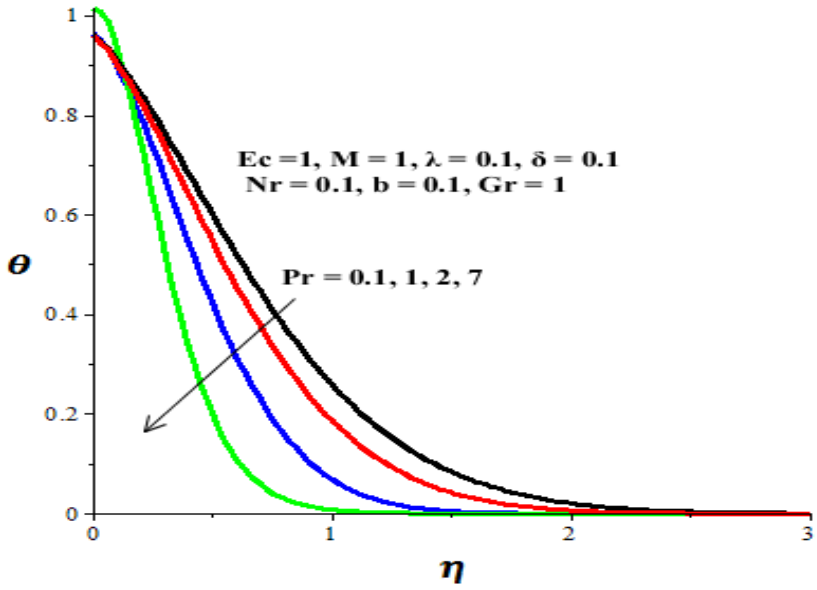

Figure (5.13): Temperature profiles with increasing *Pr*.

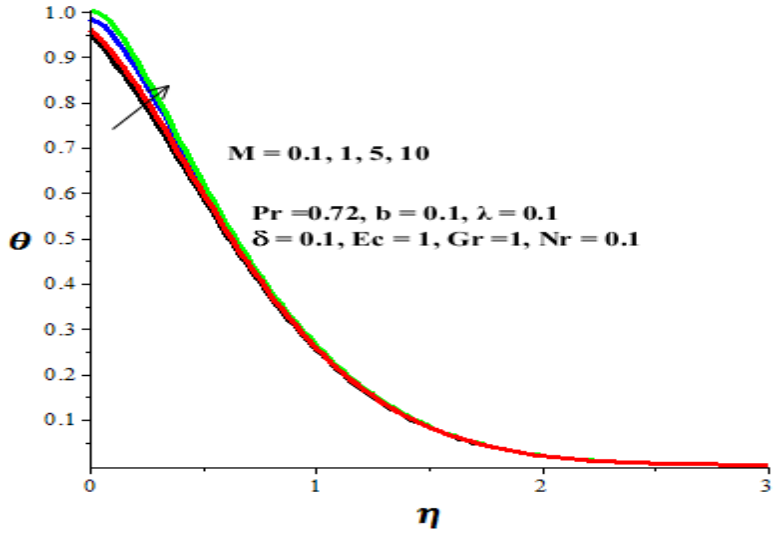

Figure (5.14): Temperature profiles with increasing *M*.

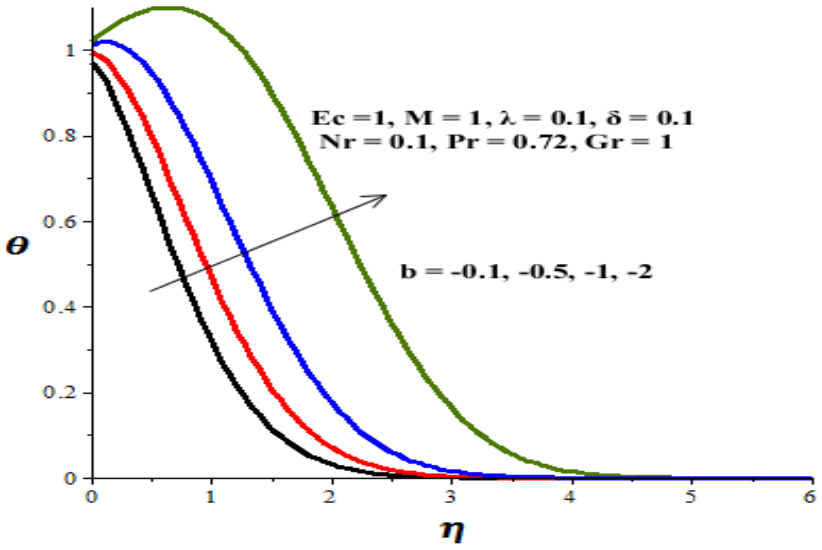

Figure (5.15): Temperature profiles with increasing injection ($b < 0$).

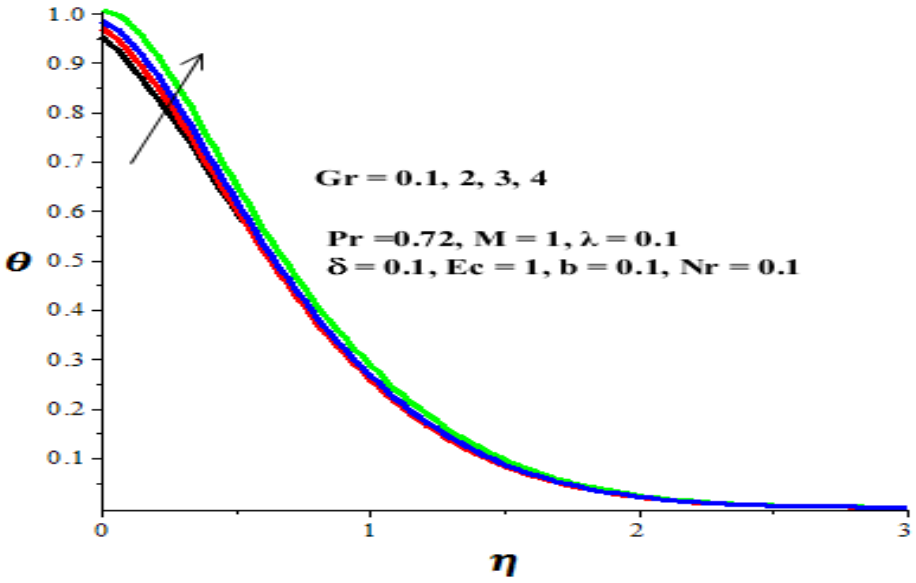

Figure (5.16): Temperature profiles with increasing Gr.

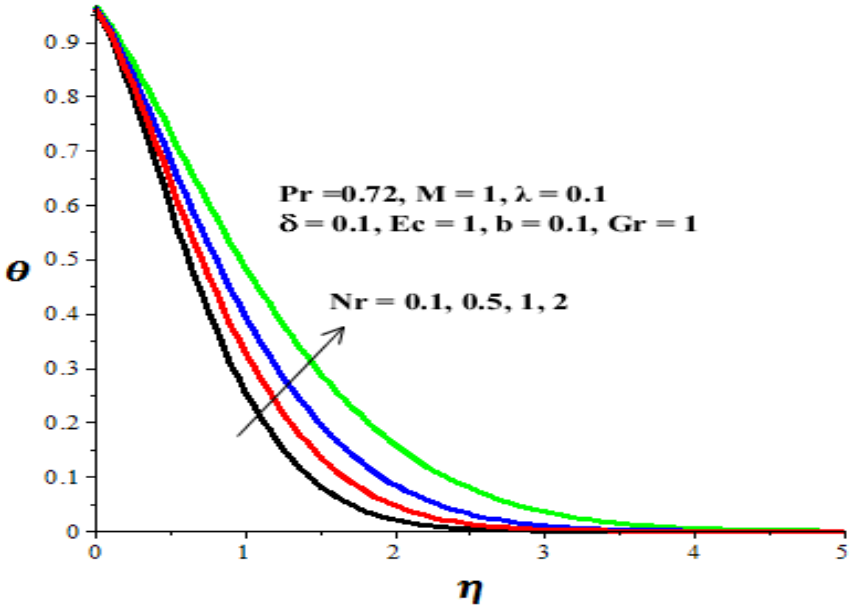

Figure (5.17): Temperature profiles with increasing *Nr*.

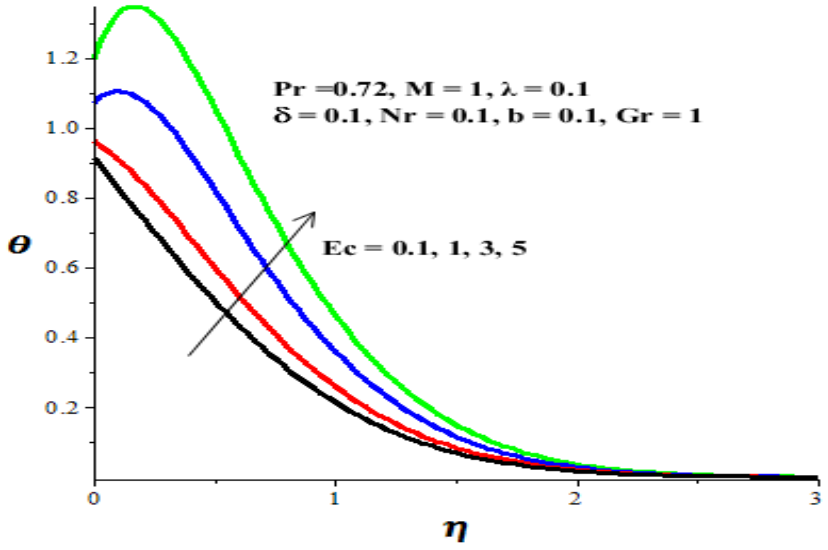

Figure (5.18): Temperature profiles with increasing *Ec*.

5.3 Skin Friction and Nusselt Number

Figures 5.19-5.24 give the distribution of the skin friction coefficient and Nusselt number at the plate surface for various thermophysical parameter values. One can note from **Figure 5.19** that the skin friction coefficient increases with an increase in magnetic field intensity (*M*), Grashof number (*Gr*) and Eckert number (*Ec*). This may be attributed to a rise in the velocity gradient at the plate surface due to momentum gain produced by Lorentz force, thermal buoyancy and viscous dissipation in boundary layer. **Figure**s 5.20-5.21 show that the skin friction coefficient increases with an increase in fluid suction, velocity slip and thermal radiation absorption but decreases with an increase in fluid injection, temperature jump and Prandtl number. This increase or decrease in the skin friction coefficients can be attributed to a decrease or increase in the velocity gradient at the plate surface as these parameters increase. Moreover, it is noted that, in the slip flow regime, shear stress adjacent to the surface can be manipulated through suction/injection parameter. **Figures** 5.22-5.24 exhibit the effects of thermophysical parameters variation on the plate surface heat transfer rate. An increase in the magnetic field intensity (*M*), Grashof number (*Gr*) and Eckert number (*Ec*) causes a decrease in the surface heat transfer rate as shown in **Figure** 5.22. This is expected, since a rise in the fluid temperature due to *M*, *Gr* and *Ec* increase causes a decrease in the temperature gradient at the plate surface, consequently, the Nusselt number decreases. **Figure**

5.23 revealed that an increase in mass suction tends to increase the surface heat transfer rate, whereas injection acts in the opposite way. Moreover, the Nusselt number reduces with an increase in both slip coefficient and temperature jump parameter due to surface cooling. It is interesting to note that the hydrodynamic slip and temperature jump boundary conditions have capability of decreasing the heat transfer rate along stationary permeable surface. **Figure** 5.24 shows a rise in the surface heat transfer rate as the thermal radiation absorption parameter (*Nr*) and Prandtl number (*Pr*) increase. As expected, increase in Nr represents a rise in the radiative heat transfer which contributes to the total heat transfer rate at the plate surface. However, a decrease in the fluid temperature due to *Pr* causes an increase in the temperature gradient at the plate surface, consequently, the Nusselt number increases.

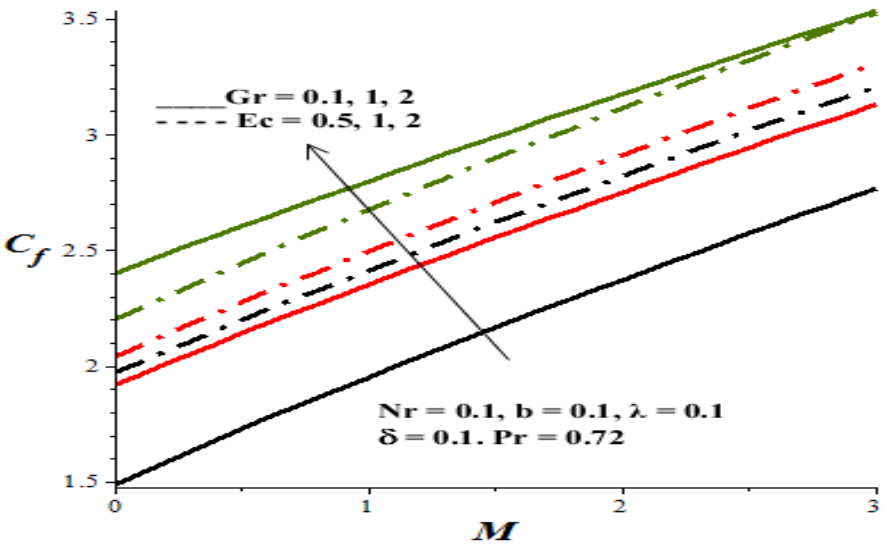

Figure (5.19): Skin friction with increasing *Ec*, *Gr* and *M*.

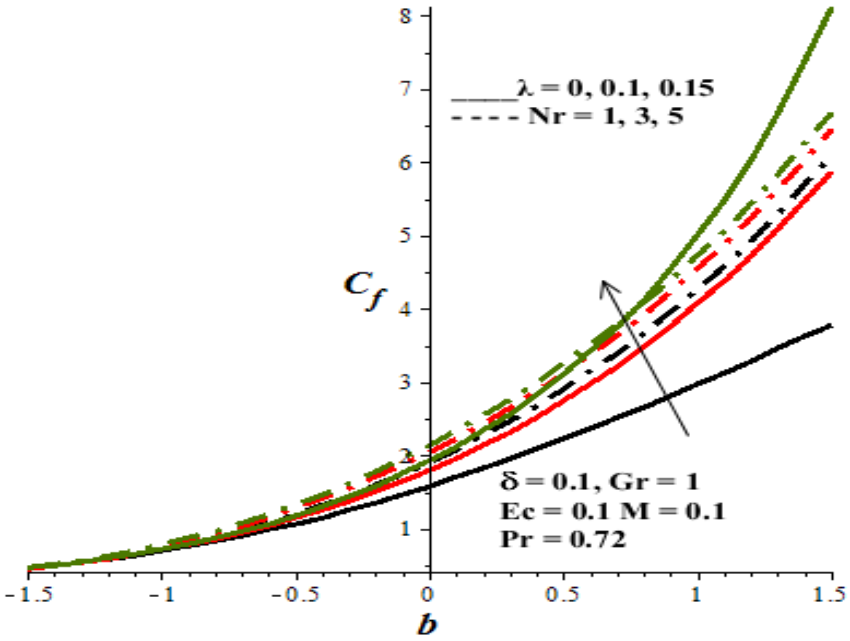

Figure (5.20): Skin friction with increasing *Nr*, λ and *b*.

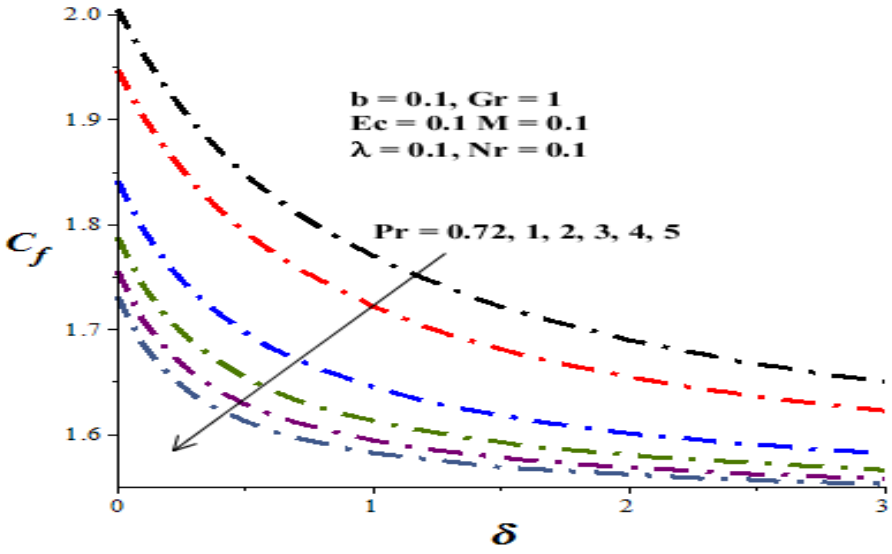

Figure (5.21): Skin friction with increasing *Pr* andδ.

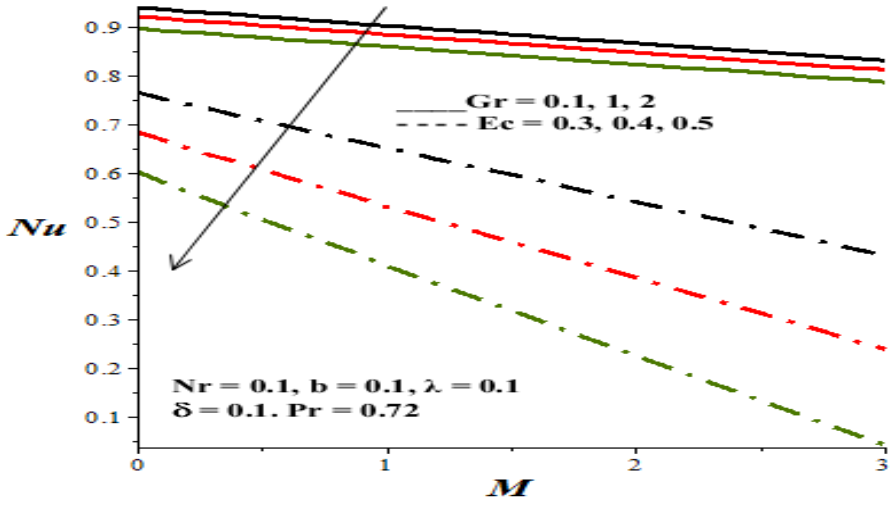

Figure (5.22): Nusselt number with increasing *Gr*, *Ec* and *M*.

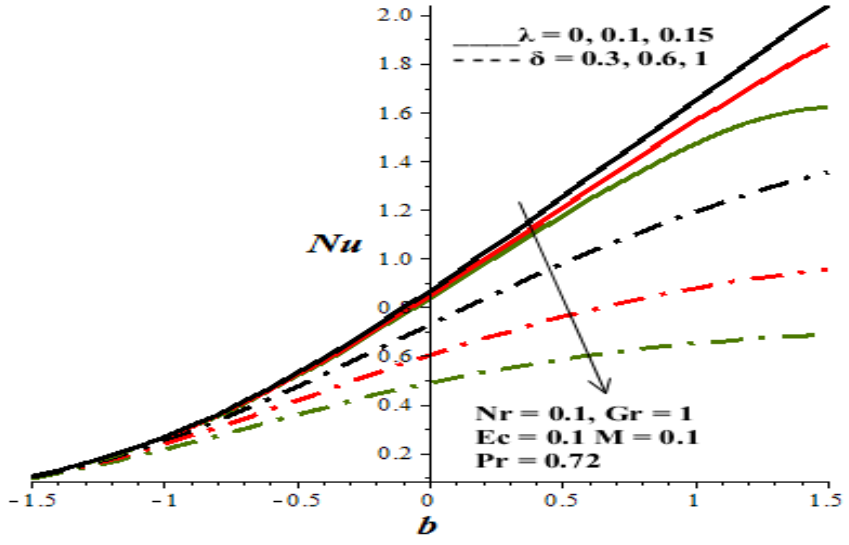

Figure (5.23): Nusselt number with increasing λ, δ and *b*.

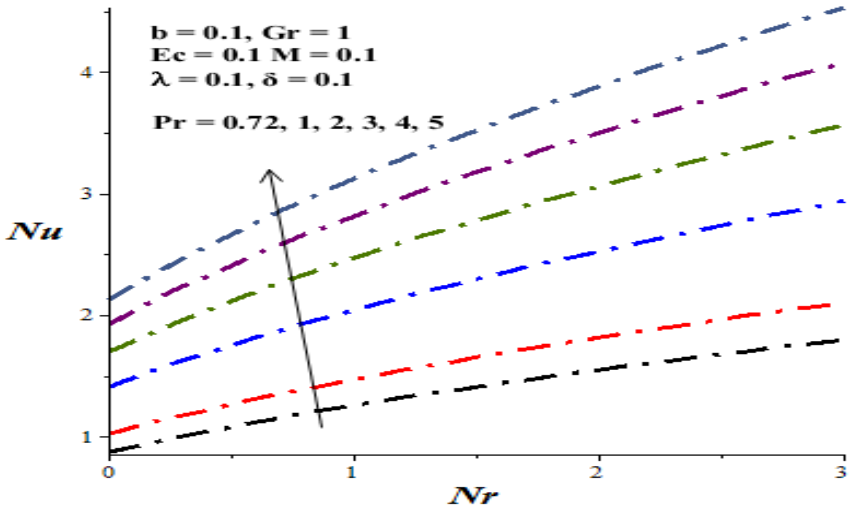

Figure (5.24): Nusselt number with increasing *Nr* and *Pr*.

5.4 Entropy Generation Rate

Figures 5.25-5.32 display the entropy generation rate for various parametric values. Generally, the entropy production attains its highest value at the permeable plate surface and gradually decreases to zero value at free stream far away from the plate surface. Interestingly, an increase in the slip coefficient, temperature jump parameter and fluid injection decreases the entropy production at the plate surface and within the boundary layer as shown in **Figure**s 5.25-5.27. Moreover, the slip coefficient, temperature jump parameter and fluid injection have decreasing effects on both fluid friction and heat transfer irreversibilities. The effect of the magnetic field parameter *M* on the entropy generation rate is shown in **Figure** 5.28. It is indicated that an increase in the *M* tends to increase the entropy production at the plate surface and within boundary layer region. This can be attributed to the fact that the magnetic field parameter has an increasing effect on the fluid friction and magneticirreversibilities. Similar trend is observed in **Figure**s 5.29-5.32. As the values of fluid suction parameter ($b>0$), Grashof number (Gr), radiation absorption parameter (Nr) and dimensionless group parameter ($Br\Omega^{1}$) increase, the entropy production at the plate surface and within the boundary layer increases. It is important to note that Grashof number (Gr), suction ($b>0$) and dimensionless group parameter $Br\Omega^{1}$ have increasing effects on fluid

friction and magnetic irreversibilities, while the radiation absorption (*Nr*) has increasing effect on the heat transfer irreversibility.

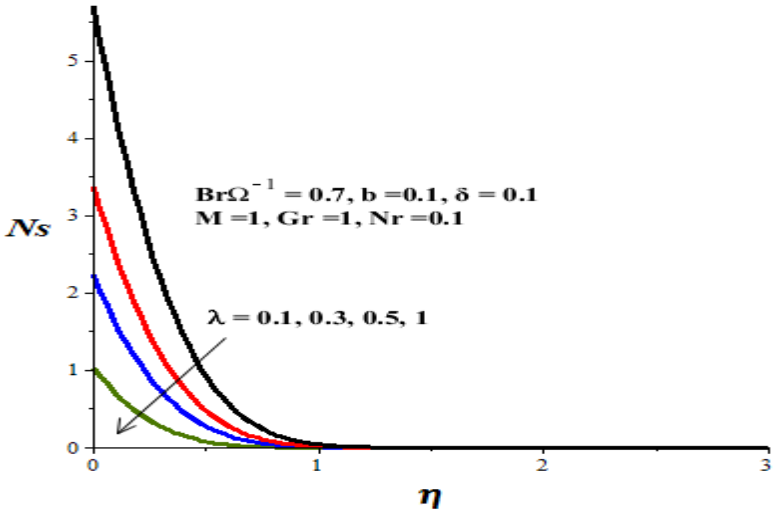

Figure (5.25): Entropy generation rate with increasing λ.

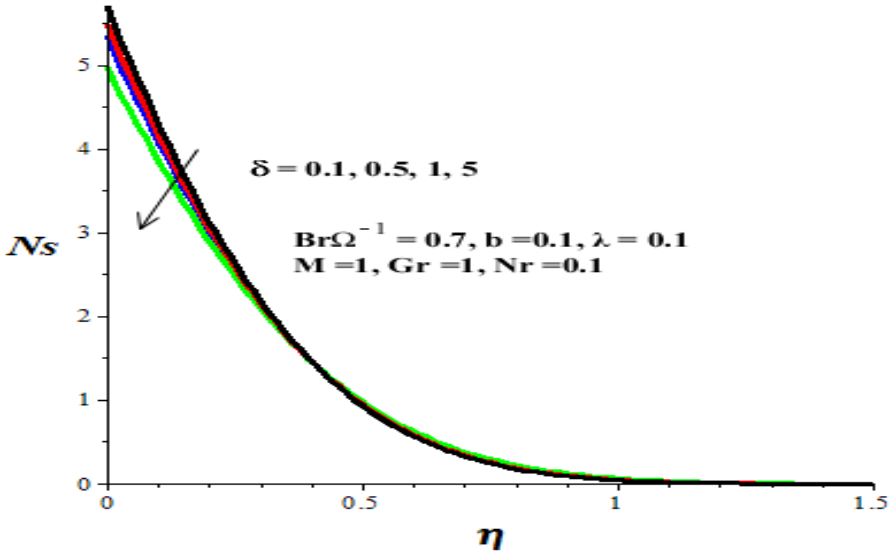

Figure (5.26): Entropy generation rate with increasing δ.

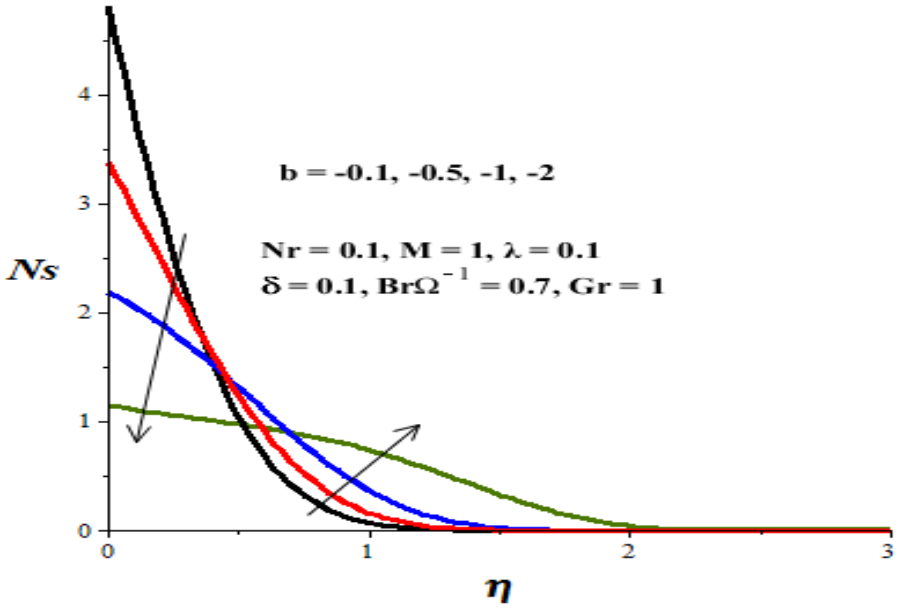

Figure (5.27): Entropy generation rate with increasing injection (b<0).

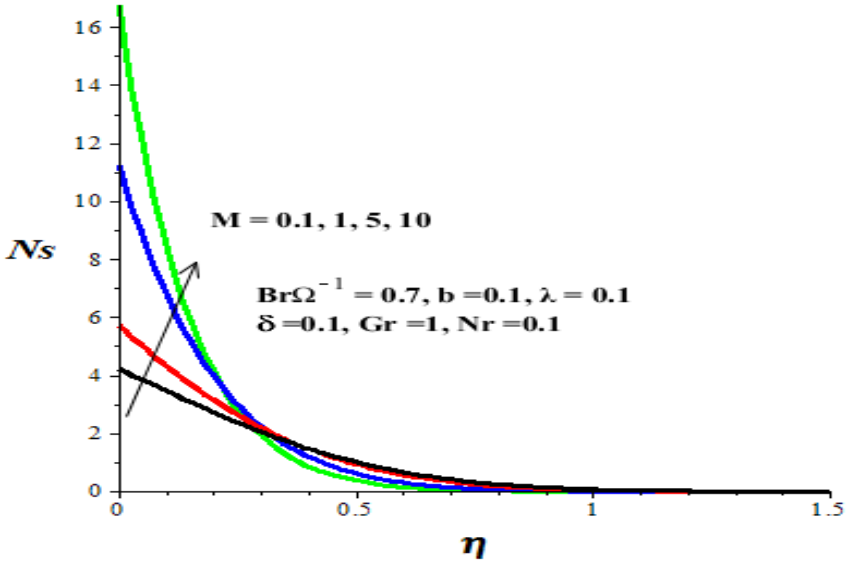

Figure (5.28): Entropy generation rate with increasing M.

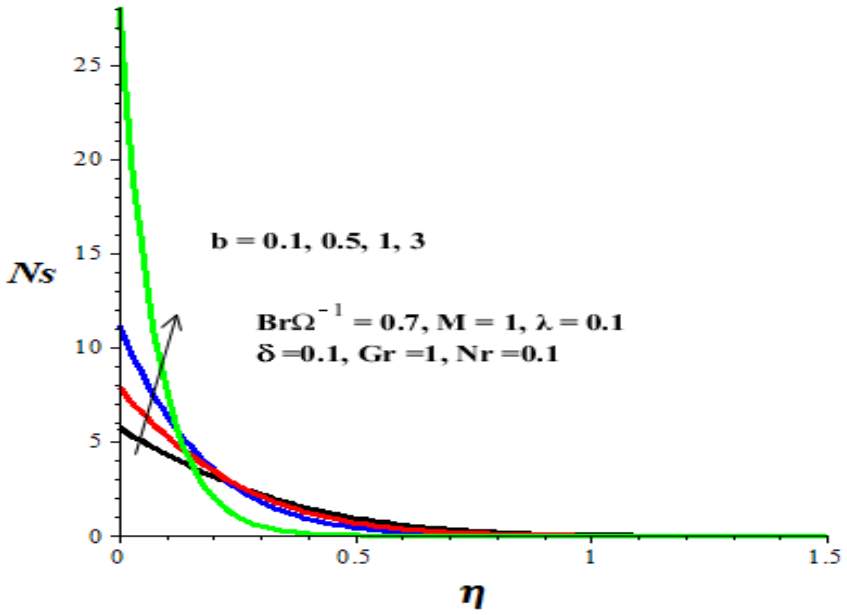

Figure (5.29): Entropy generation rate with increasing suction (b>0).

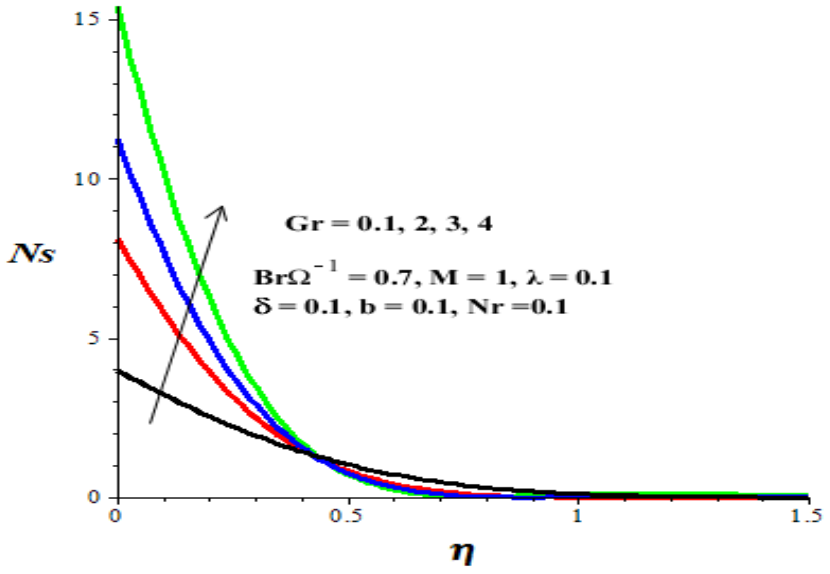

Figure (5.30): Entropy generation rate with increasing *Gr*.

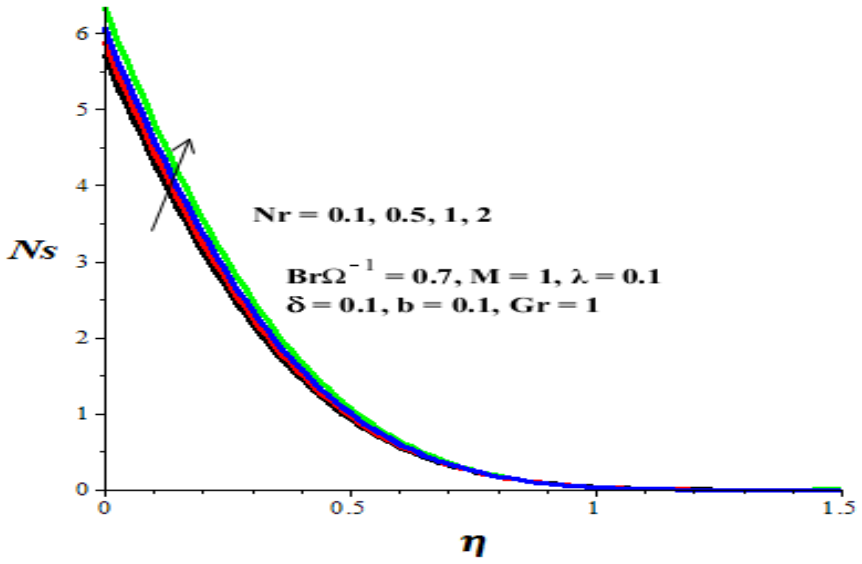

Figure (5.31): Entropy generation rate with increasing *Nr*.

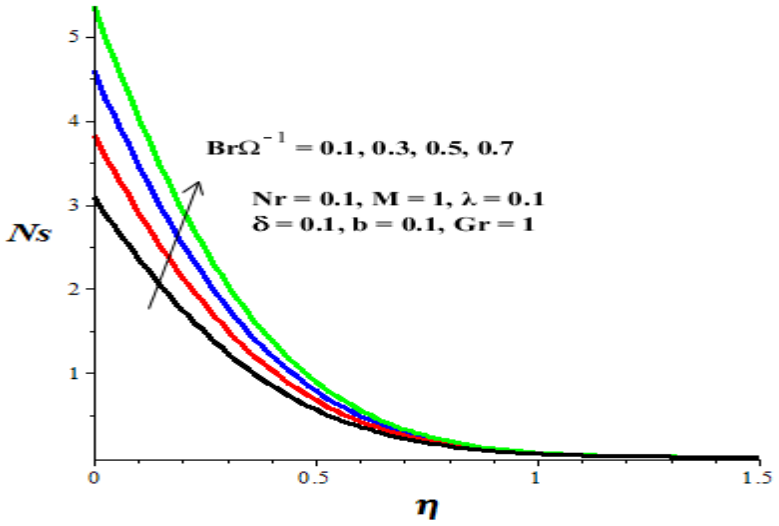

Figure (5.32): Entropy generation rate with increasing $Br\Omega^{1}$.

5.5 Bejan Number

Figures 5.33-5.40 illustrate the effects of parameter variation on Bejan (*Be*) number. Generally, Bejan number ranges from 0 to 1. It is interesting to note that the irreversibility is solely due to heat transfer and thermal radiation at the free stream when the Bejan number approaches 1 for all

parameter values, while at the permeable plate surface, the Bejan number is much less than 1 and in some cases approaches zero. This implies that the irreversibilities due to the combined effects of fluid friction and magnetic field increase their dominant at the plate surface. Moreover, as the value of slip coefficient increases (λ), the dominant effects of fluid friction and magnetic field irreversibilities at the plate surface decrease and the value of Bejan number increases above zero (see **Figure** 5.33). The irreversibility due to heat transfer and thermal radiation dominate when $Be > 0.5$. A similar trend is observed in **Figure** 5.34 with increasing Bejan number ($Be > 0$) at the plate surface as suction parameter increases. **Figures** 5.35-5.38 show the combined effects of dimensionless group parameter ($Br\Omega^{1}$), temperature jump parameter (δ), radiation absorption parameter (Nr) and fluid injection parameter ($b < 0$) on the Bejan number at the plate surface and within the boundary layer region. It is observed that as these parameters increase, the Bejan number at the plate surface tends to zero, consequently, the entropy generation due to the combined effects of fluid friction and magnetic field are dominant. It can also be observed from **Figure**s 5.39-5.40 that the Bejan number decreases to zero at the plate surface with increasing magnetic field intensity (M) and thermal buoyancy (Gr), consequently, fluid friction and magnetic field irreversibilities dominate. Finally, it is noteworthy that the plate surface acts as a strong source of irreversibility. The entropy generation within the boundary layer region can be attributed to the combined action of heat transfer, thermal radiation and fluid friction and magnetic field irreversibilities.

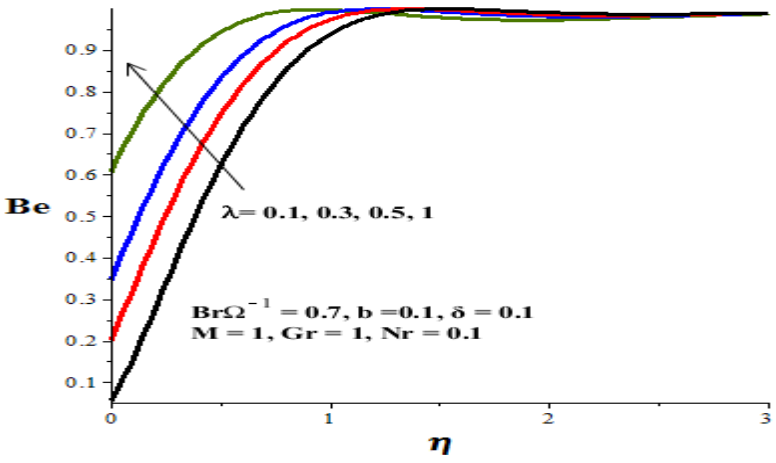

Figure (5.33): Bejan number with increasing λ.

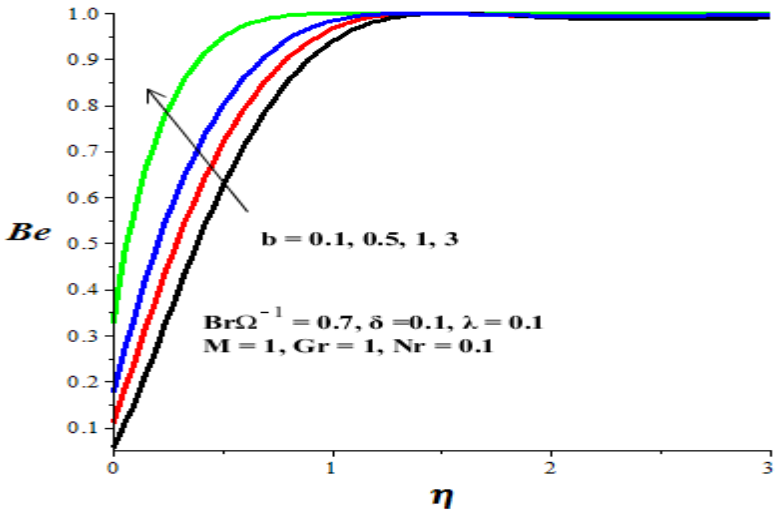

Figure (5.34): Bejan number with increasing suction (b>0).

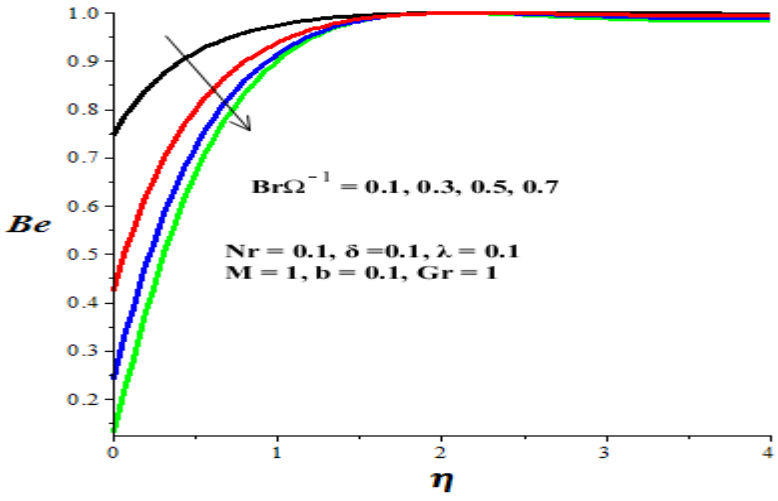

Figure (5.35): Bejan number with increasing $Br\Omega^{-1}$.

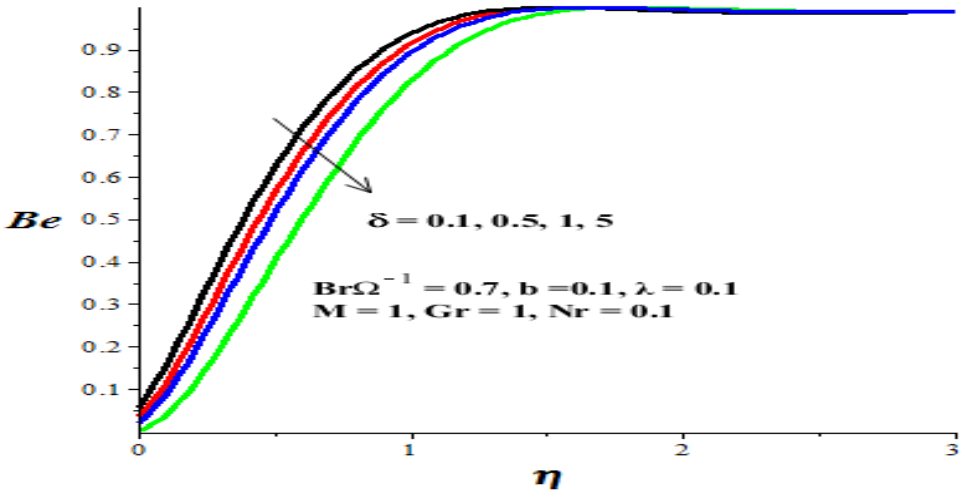

Figure (5.36): Bejan number with increasing δ.

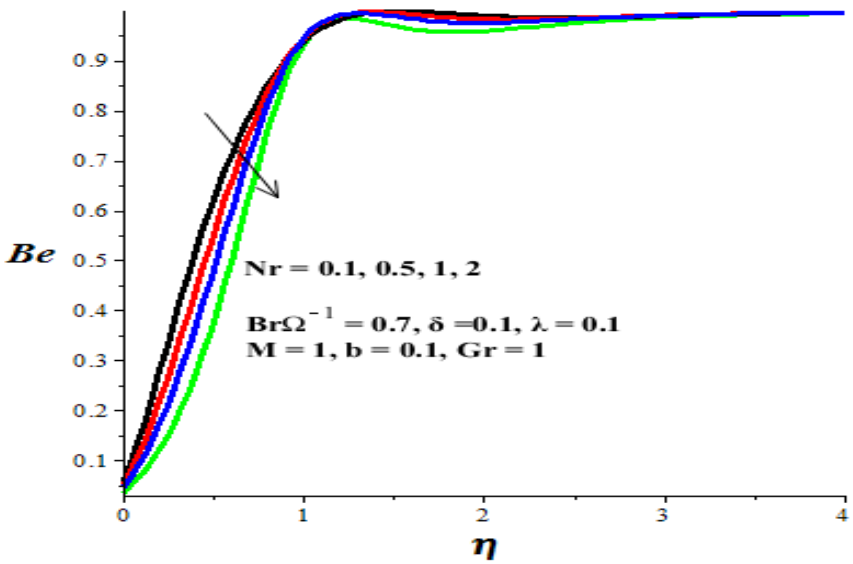

Figure (5.37): Bejan number with increasing *Nr*.

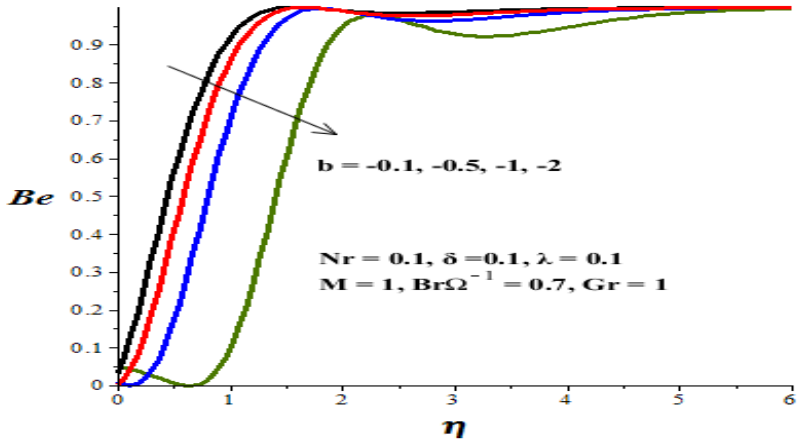

Figure (5.38): Bejan number with increasing injection ($b< 0$).

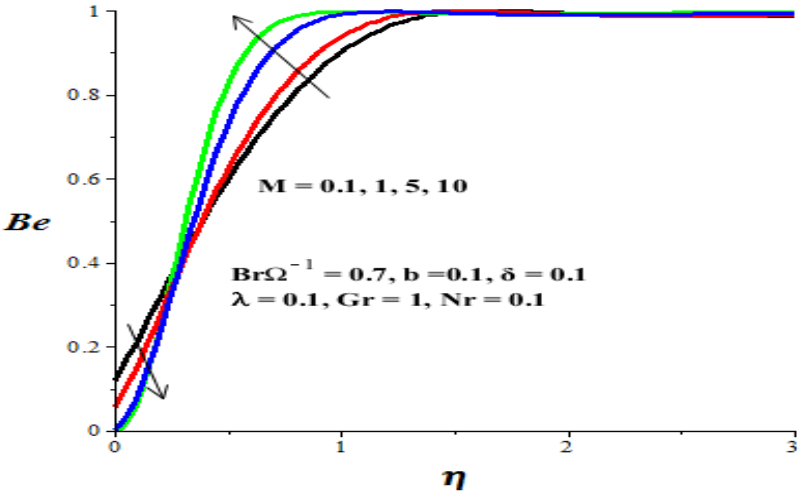

Figure (5.39): Bejan number with increasing M.

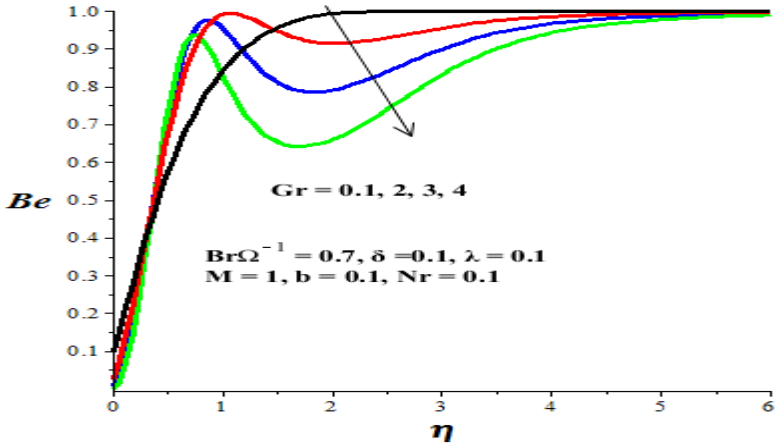

Figure (5.40): Bejan number with increasing *Gr*.

5.6 Conclusions

The entropy generation rate in an unsteady mixed convection flow of an electrically conducting and thermally radiating fluid past a permeable vertical surface subjected to a combined action of a transverse magnetic field, Joule heating, viscous dissipation, buoyancy force, velocity slip and temperature jump is analysed. The prescribed free stream velocity outside the boundary layer is also affected by a magnetic field; consequently, the Lorenz force can push the fluid forward to accelerate the fluid motion. Using similarity variables, the model partial differential equations are transformed into a set of nonlinear coupled ordinary differential equations and solved numerically using the shooting technique coupled with Runge-Kutta Fehlberg integration technique. Graphical results are presented for the fluid velocity and temperature profiles, local skin friction coefficient and local Nusselt number, entropy generation rate and Bejan number. The main findings can be summarized as follows:

- The momentum boundary layer thickness increases with an increase in Pr, δ and $b< 0$ but decreases with an increase in M, Gr, Nr, Ec, λ and $b>0$.
- The thermal boundary layer thickness increases with an increase in M, Gr, Nr, Ec and $b<0$ but decreases with an increase in λ, δ Pr and $b>0$.
- The local skin friction coefficient increases with an increases in M, Gr, Nr, Ec, λ and $b > 0$, but decreases with an increase in Pr, δ and $b< 0$.
- The local Nusselt number increases with an increases in Pr, Nr and $b> 0$, but decreases with an increase in M, Gr, δ, Ec, λ and $b<0$.
- The entropy production at the plate surface increases with an increase in M, Gr, Nr, $Br\Omega^{1}$ and $b > 0$ but decreases with an increase in δ, λ and $b< 0$.
- Heat transfer and thermal radiation irreversibility solely dominate the free stream with Bejan number of 1 while at the plate surface the irreversibilities due to both fluid friction and magnetic field dominates with Bejan number approaching zero as $b< 0$, M, δ, Gr, Nr, $Br\Omega^{1}$ increasing and λ, $b> 0$ decreasing.

Finally, it is evident that the entropy generation rate in unsteady hydromagnetic mixed convective flow over a permeable slippery surface with thermal radiation can be sufficiently reduced using appropriate combination of thermophysical parameter values for efficient operation. Moreover, the above results can be applied to improve the design of a variety of flow and thermal systems

including micro scale systems such as micromixing technologies. It is hoped that the present work will serve as a stimulus for experimental work which appears to be lacking at present.

5.7 Study Limitation and Future Work

This study only considered the problem in time and a one dimensional space variable. This model could be extended to time and two, or three dimensional variables for an incompressible Newtonian fluid and heat transfer model. The case of non-Newtonian fluid model can also be considered within this MHD boundary layer flow framework.

REFERENCES

[1] Nisar, A., Afzulpurkar, N., Mahaisavariya, B., Tuantranont, A., MEMS-based micropumps in drug delivery and biomedical applications. Sens. Actuators B Chem. Vol. 130, 917–942, 2008.

[2] Capretto, L., Cheng, W., Hill, M., Zhang, X., Micromixing within microfluidic devices. Top. Curr. Chem., Vol. 304, 27–68, 2011.

[3] Kleinstreuer, C., Li, J., Koo, J., Microfluidics of nano-drug delivery. Int. J. Heat Mass Trans., Vol. 51, 5590–5597, 2008.

[4]Tretheway, D.C., Meinhart, C.D., A generating mechanism for apparent fluid slip in hydrophobic microchannels. Phys. Fluids, Vol.16, 1509–1515, 2004.

[5]Sparrow E. M, Eckert, E. R., Minkowycz, W. J., Transpiration cooling in a magnetohydrodynamic stagnation-point flow. Appl Sci Res A Vol.11, 125–147, 1962.

[6] Rosseland, S., Theoretical astrophysics. Oxford University, New York, NY, USA, 1936.

[7]Makinde, O. D., Ogulu, A., The effect of thermal radiation on the heat and mass transfer flow of a variable viscosity fluid past a vertical porous plate permeated by a transverse magnetic field. Chemical Engineering Communications, Vol.195 (12), 1575 -1584, 2008.

[8]Makinde, O. D., Free-convection flow with thermal radiation and mass transfer past a moving vertical porous plate. International Communications in Heat and Mass transfer, Vol. 32, 1411-1419, 2005.

[9]Cramer, K. R., Pai, S. I., Magnetofluid dynamics for engineers and applied physicists. McGraw–Hill, New York, 1973.

[10]Makinde, O. D., Onyejekwe, O. O., A numerical study of MHD generalized Couette flow and heat transfer with variable viscosity and electrical conductivity. Journal of Magnetism and Magnetic Materials, Vol.323, 2757–2763, 2011.

[11] Makinde, O. D., Chinyoka, T., Numerical investigation of buoyancy effects on hydromagnetic unsteady flow through a porous channel with suction/injection. Journal of Mechanical Science and Technology, Vol. 27 (5), 1557-1568, 2013.

[12]Makinde, O. D., Khan, W. A., Culham, J. R., MHD variable viscosity reacting flow over a convectively heated plate in a porous medium with thermophoresis and radiative heat transfer. International Journal of Heat and Mass Transfer, Vol.93, 595–604, 2016.

[13] Mukhopadhyay, S., Slip effects on MHD boundary layer flow over an exponentially stretching sheet with suction/blowing and thermal radiation. Ain Shams Eng. J., Vol.4 (3), 485-491, 2013.

[14]Sharma, P.R., Singh, G., Effects of variable thermal conductivity, viscous dissipation on Steady MHD natural convection flow of low Prandtl fluid on an inclined porous plate with Ohmic heating. Meccanica, Vol.45, 237- 247, 2010.

[15] Kim, Y.J., Unsteady MHD convective heat transfer past a semi-infinite vertical porous moving plate with variable suction. International Journal of Engineering Science, Vol.38, 833-845, 2000.

[16] Bhattacharyya, K., Layek, G. C., Chemically reactive solute distribution in MHD boundary layer flow over a permeable stretching sheet with suction or blowing. Chem. Eng. Commun., Vol.197, 1527-1540, 2010.

[17] Zheng, L., Niu, J., Zhang, X., Gao, Y., MHD flow and heat transfer over a porous shrinking surface with velocity slip and temperature jump. Math. Comp. Model., Vol. 56, 133-144, 2012.

[18] *Lieb, E. H., Yngvason, J., The physics and mathematics of the second law of thermodynamics. Physics Reports Vol. 310, 1–96, 1999.*

[19] Bejan, A., A study of entropy generation in fundamental convective heat transfer. J. Heat Transfer, Vol. 101, 718-725, 1979.

[20] Bejan, A., Tsatsaronis, G., Moran, M., Thermal design and optimization, Wiley, New York, USA, 1996.

[21] Makinde, O. D., Entropy analysis for MHD boundary layer flow and heat transfer over a flat plate with a convective surface boundary condition. Int. J. Exergy, Vol.10 (2), 142-154 2012.

[22] Das, S., Chakraborty, S., Jana, R. N., Makinde, O. D.,Entropy analysis of unsteady magneto-nanofluid flow past accelerating stretching sheet with convective boundary condition. Applied Mathematics and Mechanics, Vol. 36 (12), 1593-1610, 2015.

[23] Ibáñez, G., Cuevas, S., Entropy generation minimization of a MHD flow in a microchannel. Energy, Vol. 35, 4149–4155, 2010.

[24] Woods, L. C., Thermodynamics of fluid systems. Oxford University Press, Oxford, UK, 1975.

[25] Chinyoka, T., Makinde, O. D., Analysis of entropy generation rate in an unsteady porous channel flow with Navier slip and convective cooling. Entropy, Vol. 15, 2081-2099, 2013.

[26] Mahmud, S., Fraser, R.A., Flow, thermal and entropy generation characteristic inside a porous channel with viscous dissipation. Int. J. Therm. Sci., Vol. 44, 21-32, 2005.

[27] Makinde, O. D., Beg, O. A., On inherent irreversibility in a reactive hydromagnetic channel flow. Journal of Thermal Science Vol.19 (1), 72-79, 2010.

[28] Makinde, O. D., Entropy analysis for MHD boundary layer flow and heat transfer over a flat plate with a convective surface boundary condition. International Journal of Exergy, Vol. 10 (2),142-154, 2012.

[29] Yazdi, M. H., Abdullah, S., Hashim, I., Sopian, K., Reducing entropy generation in MHD fluid flow over open parallel microchannels embedded in a micropatterned permeable surface. Entropy, Vol.15, 4822-4843, 2013.

[30] Na, T.Y.,Computational methods in engineering boundary value problem. Academic Press, 1979.

[31] Prandtl, L., Uber Flussigkeits bewegung bei sehr kleiner reibung. *Verhaldlg III Int. Math. Kong*. (Heidelberg: Teubner) pp 484–491, 1904.

[32] Prandtl, L., Der luftwiderstand von kugeln. *Nachr. Acad. Wiss. G¨ottingen, Math. Phys.* 177–190, 1914.

[33] *Blasius, H., Grenzschichten in flüssigkeiten mit kleiner reibung. Z. Angew. Math. Phys. 56: 1–37, 1908.*

[34] Schlichting H., Boundarylayertheory, Springer-Verlag, NewYork, 2000.

[35] *Alfvén, H., Existence of electromagnetic-hydrodynamic waves. Nature 150: 405–406, 1942.*

[36] Abu-Hijleh, A. Natural convection and entropy generation from a cylinder with high conductivity fins. Numer. Heat Transfer A 39 405–32, 2004.

[37] Batchelor, G. K., An introduction to fluid dynamics. Cambridge University Press, 1967.

[38] Bird, R. B., Stewart, W.E, Lightfoot, E. N., Transport phenomenon. John Wiley & Sons, 1960.

[39] Carrington, A. G., Sun, Z. F.. Second law analysis of combined heat and mass transfer in internal and external flows. Int. J. Heat Fluid Flow, 13, 65–70, 1992.

[40] Cengel, Y.A., Boles, M. A., Thermodynamics: An engineering approach. McGraw-Hill, New York, 2001.

[41] Chin, K. E., Nazar, R., Arifin, N. M., Pop, I., Effect of variable viscosity on mixed convection boundary layer flow over a vertical surface embedded in a porous medium. International Communication in Heat and Mass Transfer 34, 464-473, 2007.

[42] Douglas, J. F., Gasiorek, J. M., Swaffield, J. A., Fluids mechanics. Addison Wesley Longman Ltd., Harlow, 1995.

[43] Hyder, S. J., Yilbas B. S.. Entropy analysis of conjugate heating in a pipe flow Int. J. Energy Res. 26 253–262, 2002.

[44] Ibanez, G., Cuevas, S., Lopez de Haro, H., Minimization of entropy generation by asymmetric convective cooling. Int. J. Heat Mass Transfer 46 1321–1328, 2003.

[45] Kays, W. M., Crawford, M. E., Convective heat and mass transfer. Mcgraw-Hill, Inc., 1993.

[46] Makinde, O. D., Irreversibility analysis for gravity driven non-Newtonian liquid film along an inclined isothermal plate. Phys. Scr. 74 642–645, 2006.

[47] Makinde, O. D., Irreversibility analysis of variable viscosity channel flow with convective cooling at the walls. Can. J. Phys. 86 383–389, 2008.

[48] Makinde, O. D.,Entropy-generation analysis for variable-viscosity channel flow with non-uniform wall temperature. Applied Energy, Vol. 85, 384-393, 2008.

[49] U. Narusawa, U., The second law analysis of mixed convection in rectangular ducts. Heat Mass Transfer, 37 197–203, 2001.

[50] Sahin A. Z., Effect of variable viscosity on the entropy generation and pumping power in a laminar fluid flow through a duct subjected to constant heat flux Heat Mass Transfer, 35 499–506, 1999.

[51] White, F. M., Viscous fluid flow, 3rd Edition. McGraw-Hill, Inc., 2006.

[52] Reddy Gorla, R. S., Byrd, L. W., Pratt, D. M., Second law analysis for microscale flow and heat transfer, Applied Thermal Engineering, Vol. 27, 1414-1423, 2007.